Open access • Journal Article • DOI:10.1109/TITS.2003.821340

Analysis of traffic flow with mixed manual and semiautomated vehicles

A. Bose, Petros Ioannou

Institutions: University of Southern California

Published on: 01 Dec 2003 - IEEE Transactions on Intelligent Transportation Systems (IEEE)

Title
Analysis of Traffic Flow with Mixed Manual and Semi-automated Vehicles

Authors
Bose, Arnab
Ioannou, Petros

Publication Date
1999-05-01

CALIFORNIA PATH PROGRAM
INSTITUTE OF TRANSPORTATION STUDIES
UNIVERSITY OF CALIFORNIA, BERKELEY

Analysis of Traffic Flow with Mixed Manual and Semi-automated Vehicles

Arnab Bose, Petros Ioannou
University of Southern California

California PATH Research Report
UCB-ITS-PRR-99-14

This work was performed as part of the California PATH Program of the University of California, in cooperation with the State of California Business, Transportation, and Housing Agency, Department of Transportation; and the United States Department of Transportation, Federal Highway Administration.

Report for MOU 317

May 1999

ISSN 1055-1425

ANALYSIS OF TRAFFIC FLOW WITH MIXED MANUAL AND SEMI-AUTOMATED VEHICLES*

Arnab Bose and Petros Ioannou

Center for Advanced Transportation Technologies

Dept. of Electrical Engineering-Systems, EEB200A

University of Southern California

Los Angeles, CA 90089-2562, USA

abose@scf.usc.edu, ioannou@almaak.usc.edu

* This work is supported by the California Department of Transportation through PATH of the University of California. The contents of this paper reflect the views of the authors who are responsible for the facts and accuracy of the data presented herein. The contents do not necessarily reflect the official views or policies of the State of California or the Federal Highway Administration. This paper does not constitute a standard, specification or regulation.

ANALYSIS OF TRAFFIC FLOW WITH MIXED MANUAL AND SEMI-AUTOMATED VEHICLES

Arnab Bose and Petros Ioannou

Abstract

During the last decade considerable research and development efforts have been devoted to automating vehicles in an effort to improve safety and efficiency of vehicle following. While dedicated highways with fully automated vehicles is a far in the future objective, the introduction of semi-automated vehicles on current highways designed to operate with manually driven vehicles is a realistic near term objective. The purpose of this paper is to analyze the effects on traffic flow characteristics and environment when semi-automated vehicles with automatic vehicle following capability (in the same lane) operate together with manually driven vehicles. We have shown that semi-automated vehicles do not contribute to the slinky effect phenomenon observed in today's highway traffic when the lead manual vehicle performs smooth acceleration maneuvers. We have demonstrated that semi-automated vehicles smooth traffic flow by filtering the response of rapidly accelerating lead vehicles. The smooth response of the semi-automated vehicles designed for passenger comfort significantly reduces fuel consumption and levels of pollutants of following vehicles when the lead manual vehicle performs rapid acceleration maneuvers. We have demonstrated using simulations that the fuel consumption and pollution levels present in manual traffic simulated using a car following model that models the slinky effect behavior observed in manual driving can be reduced during rapid acceleration transients by 7.3% and 3.8%-47.3% respectively due to the presence of 10% semi-automated vehicles. Due to the randomness and uncertainties in human driving, the numbers obtained are qualitatively valid and demonstrate the beneficial effect of semi-automated vehicles in mixed traffic in improving air quality and fuel consumption.

Keywords semi-automated vehicles, mixed traffic, Intelligent Cruise Control (ICC), string stability, fuel economy, pollution

Executive Summary

In this paper, the effects of semi-automated vehicles among manual ones in mixed traffic at the microscopic level are analyzed and simulated. All vehicles are assumed to travel on a long straight road. The semi-automated vehicles are modeled using an Intelligent Cruise Control design that consists of throttle and brake subsystems. The manually driven vehicles are modeled using different human driver vehicle following models that exist in literature. We show that semi-automated vehicles in mixed traffic do not contribute to the slinky effect phenomena during smooth transients. Furthermore, semi-automated vehicles smooth traffic flow by filtering the response of rapidly accelerating lead vehicles. This is done at the expense of larger position, velocity and acceleration errors and sometimes at the expense of falling far behind the vehicle ahead. Simulations demonstrate that the presence of semi-automated vehicles in mixed traffic improves air pollution levels and fuel savings during transients caused by rapid acceleration maneuvers.

Contents

1 INTRODUCTION **1**

2 STRING STABILITY IN MIXED TRAFFIC **3**

2.1 Mathematical Definitions 3
2.2 String Stability of Manual Vehicles 9
2.3 String Stability of Semi-Automated Vehicles 14
2.4 String Stability of Mixed Vehicles 20
2.5 Simulations 26

3 ENVIRONMENTAL IMPACT OF MIXED TRAFFIC **31**

3.1 Introduction 31
3.2 Simulations 31

4 CONCLUSIONS **37**

REFERENCES **37**

List of Figures

Figure 1: Interconnected system of vehicles following each other in a single lane. 3

Figure 2: Pipes linear car following model: (a) Impulse response $g_p(t)$ vs t (b) $\int_0^t |g_p(\tau)|d\tau$ vs t and (c) $|G_p(j\omega)|$ vs ω 11

Figure 3: Optimal control car following model: (a) Response of the nonlinear model to an impulse function, (b) impulse response $g_o(t)$ vs t and (c) $|G_o(j\omega)|$ vs ω when the model is linearized around the operating speed of 15m/s. 13

Figure 4: Look ahead car following model: (a) Impulse response $g_{l1}(t)$ vs t (b) $\int_0^t |g_{l1}(\tau)|d\tau$ vs t and (c) $|G_{l1}(j\omega)|$ vs ω. 15

Figure 5: Throttle controller subsystem: (a) Impulse response $g_{th}(t)$ vs t (b) $\int_0^t |g_{th}(\tau)|d\tau$ vs t and (c) $|G_{th}(j\omega)|$ vs ω. 18

Figure 6: Acceleration Limiter. 19

Figure 7: Brake controller subsystem: (a) Impulse response $g_{br}(t)$ vs t (b) $\int_0^t |g_{br}(\tau)|d\tau$ vs t and (c) $|G_{br}(j\omega)|$ vs ω. 21

Figure 8: Mixed manual/semi-automated traffic. 22

Figure 9(a): Area under the curve of $g_{ii-1}(t)$ as a function of semi-automated vehicle headway from 0.5s to 1.5s for different manual vehicle headways of 1.0s, 1.8s and 2.2s. 25

Figure 9(b): $\|g_{ii-1}\|_1$ as a function of semi-automated vehicle headway from 0.5s to 1.5s for different manual vehicle headways of 1.0s, 1.8s and 2.2s. 25

Figure 9(c): $\|g_{ii-1}\|_1$ as a function of manual vehicle headway from 0.6s to 2.2s for different semi-automated vehicle headways of 0.5s, 1.0s and 1.5s. 25

Figure 10: 10 vehicles in manual traffic (Pipes model) following a lead vehicle. 27

(a) Velocity response of leader (L), 1st vehicle (v1) and vehicles 3 to 5 (v3-v5) and 9,10 (v9, v10); (b) position error of vehicles 3 to 5 (v3-v5) and 9,10 (v9, v10). 27

Figure 11: 10 vehicles in mixed manual (Pipes model)/semi-automated traffic following a lead vehicle performing smooth acceleration maneuvers. The 4th vehicle (v4) is semi-automated.(a) Velocity response of leader (L), 1st vehicle (v1) and vehicles 3 to 5 (v3-v5) and 9,10 (v9, v10); (b) position error of vehicles 3 to 5 (v3-v5) and 9,10 (v9, v10). 29

Figure 12: 10 vehicles in mixed manual (Pipes model)/semi-automated traffic following a rapidly accelerating lead vehicle. The 4th vehicle (v4) is semi-automated. 30

(a) Velocity response of leader (L), 1st vehicle (v1) and vehicles 3 to 5 (v3-v5) and 9,10 (v9, v10); (b) position error of vehicles 3 to 5 (v3-v5) and 9,10 (v9, v10). 30

Figure 13: Maps for (a) CO emission and (b) NO_x emission indexed by velocity and acceleration. 32

Figure 13: Maps for (c) HC emission and (d) fuel consumption indexed by velocity and acceleration. 33
Figure 14: 10 manually driven vehicles follow a rapidly accelerating leader. Velocity response of leader (L), first vehicle (v1) and vehicles 3-5 (v3-v5) and 9,10 (v9, 10). 34
Figure 15: Total (a) CO emission and (b) NO_x emission from a string of 10 vehicles. Manual is when all vehicles are manually driven (Pipes model). Mixed is when the 4^{th} vehicle is semi-automated. 35
Figure 15: Total (c) HC emission and (d) fuel consumption from a string of 10 vehicles. Manual is when all vehicles are manually driven (Pipes model). Mixed is when the 4^{th} vehicle is semi-automated. 36

List of Tables

Table 1: Percentage savings in pollution emission and fuel consumption for mixed traffic over manual traffic. 34

1 Introduction

Recent advances in technology have propelled efforts to automate vehicles in order to achieve safe and efficient use of the current highway system. Fully automated vehicles that are able to operate autonomously in a highway environment are a long term goal. On the other hand, partially or semi-automated vehicles designed to operate with current manually driven vehicles in today's highway traffic are seen as a more near term objective. Their gradual penetration into the current highway system will usher the stage of mixed traffic where semi-automated vehicles will coexist with manually driven ones.

Considering the current penetration of products such as Anti-Lock Braking Systems (ABS), air bags and cruise control into the vehicle market, it is justifiable to expect that Intelligent Cruise Control (ICC) systems that give vehicles the capability to follow each other automatically in the same lane, will be deployed in the US in the near future. Several major car manufacturers in Japan are already producing vehicles for sale with an ICC option. ICC is the next step to cruise control. It allows a vehicle to automatically follow another vehicle in a single lane using automatic throttle and brake controllers [1] in conjunction with various on-board sensors [15]. We refer to vehicles with ICC capability as semi-automated vehicles since they provide automation only in the longitudinal direction [2]. The driver is still responsible for lateral control of the semi-automated vehicle. In the initial stages, ICC may be designed as a driver assist device and the driver will be responsible for crucial tasks like collision avoidance. Such a system may require the use of a fairly large intervehicle spacing (compared to the average used in today's driving) in an effort to account for possible larger driver reaction times due to the use of automation. As drivers become accustomed to the system and human factors and technical issues are resolved, ICC could be upgraded to have a longitudinal frontal collision avoidance (FCA) system [3]. In that case the intervehicle spacing could be reduced considerably which could result into significant improvements in highway capacity.

Human factor considerations dictate that the response of an ICC vehicle should be smooth. As a result an ICC vehicle is expected to act as a filter in vehicle following attenuating disturbances and smoothing traffic flow. Meanwhile, the vehicle-highway system is one of the major contributors to air pollution in urban areas due to increasing vehicle miles traveled and congestion [5]. With the gradual penetration of semi-automated vehicles into manual traffic, the question is whether the different dynamical response of semi-automated vehicles will have any impact on the environment and characteristics of traffic flow.

In this paper we examine the effect of semi-automated vehicles on the transient behavior of traffic flow at the microscopic level when they operate together with manually driven vehicles. In our analysis we consider three different human driver car following models [8,9,10,11,12] and a model of a semi-automated vehicle [1]. These models are used to analyze the transient behavior during vehicle following for three different cases. In case 1 all vehicles are manually driven. In case 2 all vehicles are semi-automated and in case 3 manual and semi-automated vehicles are mixed.

We have shown that in manual driving, only one car following model namely Pipes model [8,9] models slinky-type effects [6], a phenomenon observed in today's traffic. The other two human driver models model smooth driving and are shown to be free of slinky-type effects. The Pipes model was therefore used to examine the effect of mixing manually driven and semi-automated vehicles on the traffic flow characteristics during transients. The semi-automated vehicle is designed to provide smooth driving at all times with the exception of emergencies. It is free of slinky-type effects and guarantees accurate position and velocity tracking when the response of the vehicle in front is "smooth". When the response of the vehicle in front is "rough", i.e. it exhibits rapid acceleration, the semi-automated vehicle is designed to filter such response in an effort to maintain smooth driving. This is done at the expense of larger position, velocity and acceleration errors and sometimes at the expense of falling far behind the vehicle ahead.

Our analysis with mixed traffic shows that "smooth" acceleration maneuver exhibited by a lead vehicle propagates upstream and gets amplified leading to the slinky effect phenomenon. In this case the semi-automated vehicles do not contribute to the slinky effect since they are designed to respond to any smooth acceleration/velocity response in an accurate manner. When the lead vehicle exhibits a "rough" acceleration maneuver the semi-automated vehicle in a mixed traffic situation acts as a filter by converting the "rough" acceleration response to a smooth response. We have shown that this characteristic of the semi-automated vehicle has a very beneficial effect on fuel economy and pollution during rapid acceleration transients. Simulations are used to quantify these benefits using Pipes model [8,9] and the ICC model developed in [1]. We demonstrate that the fuel consumption and pollution levels present in manual traffic represented by Pipes linear car following model can be reduced during rapid acceleration transients by 7.3% and 3.8%-47.3% respectively due to the presence of 10% semi-automated vehicles.

The paper is organized as follows. In section 2 we outline the concept of string stability in vehicle following and analyze the different human driver car following and semi-automated vehicle models for string stability. We then extend our analysis into the case of mixed manual/semi-automated vehicles. Then we perform simulations for different car following scenarios in manual and mixed traffic and confirm the analytical findings. Section 3 contains a discussion of environmental impact analysis and vehicle emission maps that are used followed by simulations to illustrate the environmental benefits of semi-automated vehicles among manual ones in mixed traffic. Section 4 contains conclusions derived from our analysis.

2 String Stability in Mixed Traffic

In vehicle following the dynamics of each vehicle are coupled with other vehicles leading to a larger dynamical system. Even though each vehicle may have stable behavior and good performance, the behavior of the overall coupled system may not be desirable. For example, transients caused by a single vehicle changing its speed may be amplified upstream leading to what is known as "slinky-type effect" [6] or string instability. String stability [17] in vehicle following implies that any nonzero position, velocity and acceleration error of an individual vehicle in a string of vehicles does not get amplified as it propagates upstream. We begin by giving the mathematical definitions of string stability for interconnected systems of vehicles closely following each other in a single lane. Next, microscopic human driver car following and semi-automated vehicle models are used to investigate string stability in manual, semi-automated and mixed traffic situations. Finally, we perform a series of simulations to illustrate different manual and mixed traffic vehicle following scenarios.

2.1 Mathematical Definitions

A system of vehicles in a single lane under moderately dense traffic conditions can be considered as a countable infinite interconnected system. For simplicity, i.e. to avoid boundary conditions, we consider the system to consist of infinite subsystems. If a system comprises of finite number of subsystems, it can be treated as if the number were infinite by assuming fictitious subsystems at both ends. Such a system shown in fig 1 can be modeled as [18]

$$v_i = G_i(s)v_{i-1} \tag{1}$$

where $i \in N$, the infinite set of vehicles considered, v_i is the velocity of the ith vehicle and $G_i(s)$ is a proper stable transfer function that represents the input-output behavior of the ith vehicle. The system represents traffic in a single lane without passing in which every vehicle tries to match the speed of a preceding vehicle with some precision and intervehicle spacing. There may be nonlinear models describing such a system. Such models are linearized about an operating speed to put them in the framework of (1). Another point is that (1) describes the relationship between the vehicle of interest and the vehicle whose speed is being tracked. This need not be the immediate preceding vehicle, as it might be that the vehicle i is tracking vehicle i-2. Then (1) needs to be changed accordingly. Furthermore, (1) describes a relationship between following vehicles in the longitudinal direction and is applicable only for straight roads.

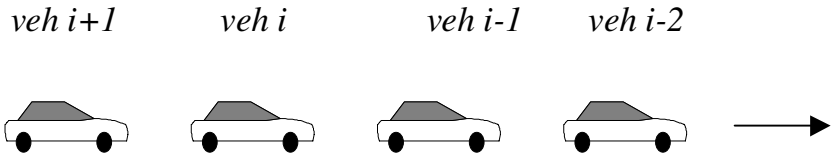

Figure 1: Interconnected system of vehicles following each other in a single lane.

Let us define the following errors for the *i*th vehicle as

$$\delta_i = x_{i-1} - x_i - L_i \qquad \text{(position error)}$$

$$v_{ri} = v_{i-1} - v_i \qquad \text{(velocity error)}$$

$$a_{ri} = a_{i-1} - a_i \qquad \text{(acceleration error)}$$

where x_i denotes the abscissa of the rear bumper of the *i*th vehicle
L_i is the constant intervehicle spacing followed by the *i*th vehicle, measured from the rear of the *i*-1 th vehicle to the rear of the *i*th vehicle
v_i denotes the velocity of the *i*th vehicle
a_i denotes the acceleration of the *i*th vehicle

Definition 1 (String Stability): The interconnected system of vehicles given in (1) is *string stable* if

$$\begin{aligned} &\| \delta_i \|_p \le \| \delta_{i-1} \|_p \\ &\| v_{ri} \|_p \le \| v_{ri-1} \|_p \\ &\| a_{ri} \|_p \le \| a_{ri-1} \|_p \end{aligned} \qquad \forall\, p \in [1,\infty],\ \forall \quad i \in N \qquad (2)$$

Definition 2 (Strict String Stability): The interconnected system of vehicles given in (1) is *strictly string stable* if

$$\begin{aligned} &\| \delta_i \|_p < \| \delta_{i-1} \|_p \\ &\| v_{ri} \|_p < \| v_{ri-1} \|_p \\ &\| a_{ri} \|_p < \| a_{ri-1} \|_p \end{aligned} \qquad \forall\, p \in [1,\infty],\ \forall \quad i \in N \qquad (3)$$

Definition 3 (String Unstable): The interconnected system of vehicles given in (1) is said to be *string unstable* if it does not satisfy (2) for any $i \in N$ or for any $p \in [1,\infty]$.

Case 1: Vehicles with constant intervehicle spacing

Let us now consider a string of vehicles with different transfer functions $G_i(s)$ that satisfy (1). We have

$$\dot{\delta}_i = v_{i-1} - v_i = (1 - G_i) v_{i-1}$$

or, (assuming zero initial condition)

$$\delta_i = \frac{1}{s}(1-G_i)v_{i-1}$$

$$v_{ri} = v_{i-1} - v_i = (1-G_i)v_{i-1}$$

$$a_{ri} = \dot{v}_{ri} = \dot{v}_{i-1} - \dot{v}_i$$

or,

$$a_{ri} = s(1-G_i)v_{i-1}$$

which shows that

$$\frac{\delta_i}{\delta_{i-1}} = \frac{v_{ri}}{v_{ri-1}} = \frac{a_{ri}}{a_{ri-1}} = \frac{(1-G_i)}{(1-G_{i-1})}G_{i-1} = \overline{G_i}(s) \qquad (4)$$

Remark 1: When all the vehicles have identical input-output characteristics, i.e. $G_i(s) = G(s)$, then $\overline{G_i}(s) = G(s)$.

Instead of the constant intervehicle spacing policy, we may have vehicles with constant time headway policy, in which case L_i in the expression for the position error would be equal to $h_i\dot{x}_i$, where h_i is the time headway of the *i*th vehicle. Time headway is defined as the time it takes for the vehicle to cover the distance measured from the rear of the front vehicle to the rear of the following vehicle. It can be shown that when all the vehicles in the fleet have identical input-output characteristics, i.e. $G_i(s) = G(s)$, then equation (4) holds also for the constant time headway policy with $\overline{G_i}(s) = G(s)$. However, the case when they have different input-output characteristics warrants further investigation.

Case 2: Vehicles with constant time headway policy

Let us now consider a string of vehicles that satisfy (1). The position error for constant time headway policy is given by

$$\delta_i = x_{i-1} - x_i - h_i\dot{x}_i$$

where h_i is the time headway of the *i*th vehicle.

Using Laplace transform and assuming zero initial condition, we have

$$\delta_i = \frac{1}{s}[v_{i-1} - v_i] - h_i v_i = \frac{1}{s}[1 - G_i - sh_iG_i]v_{i-1}$$

$$v_{ri} = v_{i-1} - v_i = (1-G_i)v_{i-1}$$

$$a_{ri} = \dot{v}_{ri} = \dot{v}_{i-1} - \dot{v}_i$$

or,

$$a_{ri} = s(1 - G_i)v_{i-1}$$

which gives us

$$\frac{\delta_i}{\delta_{i-1}} = \frac{1 - G_i - sh_i G_i}{1 - G_{i-1} - sh_{i-1} G_{i-1}} G_{i-1} = \hat{G}_i(s) \tag{5}$$

and

$$\frac{v_{ri}}{v_{ri-1}} = \frac{a_{ri}}{a_{ri-1}} = \frac{(1 - G_i)}{(1 - G_{i-1})} G_{i-1} = \overline{G}_i(s)$$

Theorem 1 (String Stability): The class of interconnected systems of vehicles following each other in a single lane without passing is *string stable* if and only if the impulse response $g_i(t)$ of the error propagation transfer function $G_i(s)$, $\overline{G}_i(s)$ or $\hat{G}_i(s)$, as the case may be, for each individual vehicle in this class satisfies

$$\|g_i\|_1 \le 1 \qquad \forall \quad i \in N \tag{6}$$

Proof:

If: Assuming $\delta_i, v_{ri}, a_{ri} \in L_p$ and $g_i \in L_1$ where $i \in N$, we have from [7]

$$\begin{aligned} \|\delta_i\|_p &\le \|g_i\|_1 \|\delta_{i-1}\|_p \\ \|v_{ri}\|_p &\le \|g_i\|_1 \|v_{ri-1}\|_p \\ \|a_{ri}\|_p &\le \|g_i\|_1 \|a_{ri-1}\|_p \end{aligned} \qquad \forall\, p \in [1, \infty] \tag{7}$$

Therefore, if we have $\|g_i\|_1 \le 1 \ \ \forall \ \ i \in N$, then (2) of definition 1 is satisfied and the system is string stable.

Only If: It can be shown that if condition (6) is not met, then there exists a position error signal that will lead to string instability for a particular transfer function that does not belong to the class of systems defined in the theorem. For example, if

$$G_i(s) = \frac{s + 2}{s^2 + s + 1}$$

we have $g_i(t) = e^{-0.5t} \cos(0.87t) + 1.732 e^{-0.5t} \sin(0.87t)$

and $\|g_i\|_1 > 1$

Consider the error signal

$$\delta_{i-1}(t) = \begin{cases} 1 & 0 \le t \le t' \\ 0 & otherwise \end{cases}$$

such that $\|\delta_{i-1}\|_\infty = 1$ and $\delta_{i-1} \in L_p$. We have

$$\delta_i(t) = \int_0^t g_i(t-\tau)\delta_{i-1}(\tau)d\tau = -1.993e^{-0.5t}\cos(0.87t) + 0.004e^{-0.5t}\sin(0.87t) + 1.993, \quad t < t'$$

$$= \int_0^{t'} g_i(t-\tau)\delta_{i-1}(\tau)d\tau = -1.993e^{-0.5t}\cos(0.87t) + 0.004e^{-0.5t}\sin(0.87t)$$
$$+ 1.993e^{-0.5(t-t')}\cos(0.87(t-t')) - 0.004e^{-0.5(t-t')}\sin(0.87(t-t')), \quad t \ge t'$$

Say $t' = 10$, then we get $\|\delta_i\|_\infty \approx 2.4 > \|\delta_{i-1}\|_\infty$ which implies string instability by definition 3. Similarly it can be also shown that $\|v_{ri}\|_\infty > \|v_{ri-1}\|_\infty$ and $\|a_{ri}\|_\infty > \|a_{ri-1}\|_\infty$ for similar velocity and acceleration error signals.

✧

Remark 2: (i) We should note that the string stability theorem refers to a class of systems. For example, the class of systems characterized by $\|g_i\|_1 \le 1 \quad \forall \quad i \in N$ is string stable. The class of systems with $\|g_i\|_1 > 1$ for some i cannot be guaranteed to be string stable because we can find at least one system in this class that is string unstable. This, however, does not mean that every system with $\|g_i\|_1 > 1$ for some i is string unstable. This is due to the fact that the condition $\|g_i\|_1 \le 1$ is obtained from an inequality that could be conservative.

(ii) In addition to string stability, it is desirable to have $g_i(t) > 0 \quad \forall \quad i \in N \quad \forall t > 0$ in order to avoid oscillatory responses [6].

Lemma 1 (Strict String Stability): The class of interconnected systems of vehicles following each other in a single lane without passing is *strictly string stable* if and only if the impulse response $g_i(t)$ of the error propagation transfer function $G_i(s)$, $\overline{G_i}(s)$ or $\hat{G}_i(s)$, as the case may be, for each individual vehicle in this class satisfies

$$\|g_i\|_1 < 1 \qquad \forall \quad i \in N \tag{8}$$

Proof: It is similar to the earlier proof and is omitted.

Remark 3: For the interconnected system of vehicles that we consider in (1), the ICC of the vehicles are designed such that at steady state (zero frequency), the velocity of the following vehicle matches that of the preceding vehicle. This means that we will always have $|G_i(0)| = 1 \quad \forall \quad i \in N$.

It is also desirable to design $G_i(s)$ so that $g_i(t)$ does not change sign in order to avoid oscillatory responses in the error signals that could give rise to "stop-and-go" traffic. If the ICC controllers are designed to guarantee that $g_i(t)$ does not change sign and $|G_i(0)|=1$, then string stability is guaranteed as stated by the following lemma.

Lemma 2: Assume that $G_i(s)$ is designed so that $g_i(t)$ does not change sign and $|G_i(0)|=1$. Then the system of *N* vehicles with transfer function $G_i(s)$, $i \in N$ is string stable.

Proof:

If the impulse response $g_i(t)$ does not change sign we have

$$\|g_i\|_1 = \int_0^\infty |g_i(t)|dt = \left|\int_0^\infty g_i(t)e^{-0t}dt\right| = |G_i(0)| = 1 \tag{9}$$

Therefore, condition (2) of definition 1 is satisfied and the string of vehicles is string stable.

✧

Remark 4: A less conservative bound could be obtained in (7) when p=2. In this case we have [7]

$$\begin{aligned} \|\delta_i\|_2 &\le \|G_i(s)\|_\infty \|\delta_{i-1}\|_2 \\ \|v_{ri}\|_2 &\le \|G_i(s)\|_\infty \|v_{ri-1}\|_2 \\ \|a_{ri}\|_2 &\le \|G_i(s)\|_\infty \|a_{ri-1}\|_2 \end{aligned} \tag{10}$$

where

$$\|G(s)\|_\infty = \sup_\omega |G(j\omega)|$$

and from [7]

$$\|G_i(s)\|_\infty \le \|g_i\|_1 \tag{11}$$

Remark 5: Since $v_i = G_i(s)v_{i-1}$, it follows that for speed following matching at steady state we should have $|G_i(0)|=1$ which means that $\|G_i(s)\|_\infty \ge 1$. This in turn means that the best we can do in (10) is to design $G_i(s)$ so that $\|G_i(s)\|_\infty = 1$. Another approach is to design $G_i(s)$ so that $|G_i(0)|=1$ and $|G_i(j\omega)|<1 \quad \forall \omega > 0$. In this case we will have strict string stability ($\|\delta_i\|_2 < \|\delta_{i-1}\|_2$, $\|v_{ri}\|_2 < \|v_{ri-1}\|_2$, $\|a_{ri}\|_2 < \|a_{ri-1}\|_2$) for frequencies $|\omega| > 0$. This approach has already been used in [1,6].

Remark 6: It should be noted that our definition for string stability is conservative. In other words if (2) is violated for some *i,* that does not mean that the response of the string

of vehicles is not acceptable. The mixing of vehicles with $G_i(s)$ that satisfies for some i and violates for some other i the conditions of the string stability theorem (6) will be analyzed in section 2.4.

2.2 String Stability of Manual Vehicles

We investigate the string stability of a fleet of manual vehicles closely following each other in a single lane using the different human driver car following models that exist in literature. These models are applicable only under conditions of fairly dense traffic in which the driver generally attempts to match his velocity to the car ahead while maintaining some intervehicle spacing. The string stability theorem is used to verify if these models belong to the class of systems that guarantee string stability. We assume that all vehicles in the fleet have identical input/output characteristics and so by remark 1 we have the following:

$$\frac{\delta_i}{\delta_{i-1}} = \frac{v_{ri}}{v_{ri-1}} = \frac{a_{ri}}{a_{ri-1}} = \frac{v_i}{v_{i-1}} = G_i(s) = G(s)$$

Thus, to investigate whether the following models belong to the class of systems that guarantee string stability, we analyze the transfer function of each model that relates the velocity of the lead vehicle to that of the following vehicle.

Pipes Model

This is a linear follow-the-leader model based on car following theory that pertains to single lane dense traffic with no passing and assumes that each driver reacts to a stimulus from the vehicle ahead. The stimulus is the velocity difference and the driver responds with an acceleration command, i.e.

$$Response(t) = Sensitivity \times Stimulus(t - \tau)$$

where τ is the reaction time of the driver-vehicle system.

It can be mathematically expressed as

$$a_f = \frac{\lambda}{M}[v_l(t-\tau) - v_f(t-\tau)]$$

where v_l and v_f are the lead and following vehicle's velocities, respectively, a_f is the following vehicle's acceleration, M is the mass of the following vehicle and λ is a sensitivity factor. The dynamics of the vehicle are modeled by an integrator and the driver's central processing and neuromuscular dynamics by a constant. It was first proposed by Pipes [8] and later validated by Chandler [9].

The transfer function of the Pipes model is given by

$$G_p(s) = \frac{v_i}{v_{i-1}} = \frac{0.37e^{-1.5s}}{s + 0.37e^{-1.5s}} \tag{12}$$

Evaluating the impulse response we get $\|g_p\|_1 = 1.1$, implying that the Pipes model does not belong to the class of systems mentioned in the theorem (given by (6)) that guarantee string stability. However, we cannot confirm the existence of slinky effect. Also $g_p(t)$ changes sign for $t>0$ (fig 2), which means that the model has an oscillatory response. We also find that $|G_p(j\omega)|>1$ for very small frequencies. As we demonstrate later using simulations, a string of vehicles represented by the Pipes model exhibits string instability.

Optimal Control Model

In [10] it is assumed that the human driver mimics a linear optimal controller in performing vehicle following. The optimal controller is based on a quadratic cost function that penalizes the weighted sum of the square of the inter-vehicle spacing and the square of the relative velocity. The quadratic performance criterion function is chosen such that the following cost function is minimized

$$J = \frac{1}{2}\int_0^\infty \{[s_L(t) - s_F(t) - \lambda v_F(t)]^2 q_1 + [v_L(t) - v_F(t)]^2 q_2 + ru^2(t)\}dt$$

where λ is the chosen time headway of the vehicle and q_1, q_2, r are the associated weights.

With the supplementary assumption that the leading and following vehicle dynamics are identical, the solution of this optimization problem is the control $u(t)$ given by

$$u(t) = C_S[s_L(t) - s_F(t) - C_C v_F(t)] + C_V[v_L(t) - v_F(t)] \tag{13}$$

where subscripts 'L' and 'F' represent the leading and following vehicles respectively, and s and v stand for the distance and velocity respectively of the vehicles while C_C, C_S and C_V are constant gains. The values of these parameters were obtained from actual traffic data.

As the weights differ from driver to driver, the best the optimal controller can perform is as a controller that simulates the behavior of a particular human driver. Another drawback of this model is that it neglects the driver's reaction time, the neuromuscular dynamics and the nonlinearities of the vehicle dynamics. These reasons prompted Burnham [11,12] to first modify the optimal controller structure by introducing the effects of driver reaction time and vehicle nonlinearities and then estimate the unknown

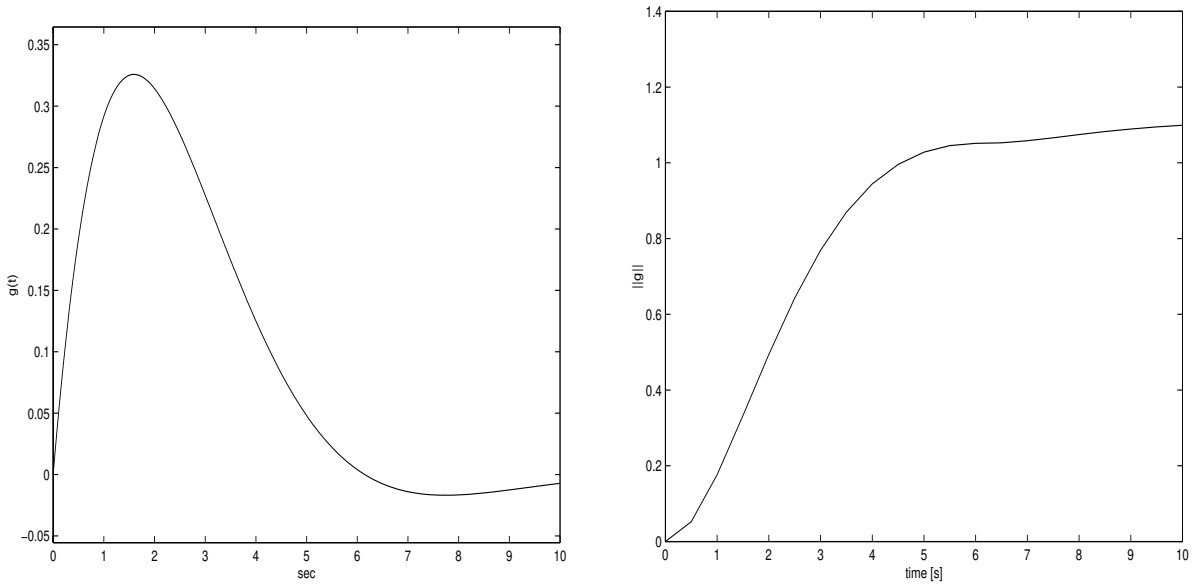

(a) (b)

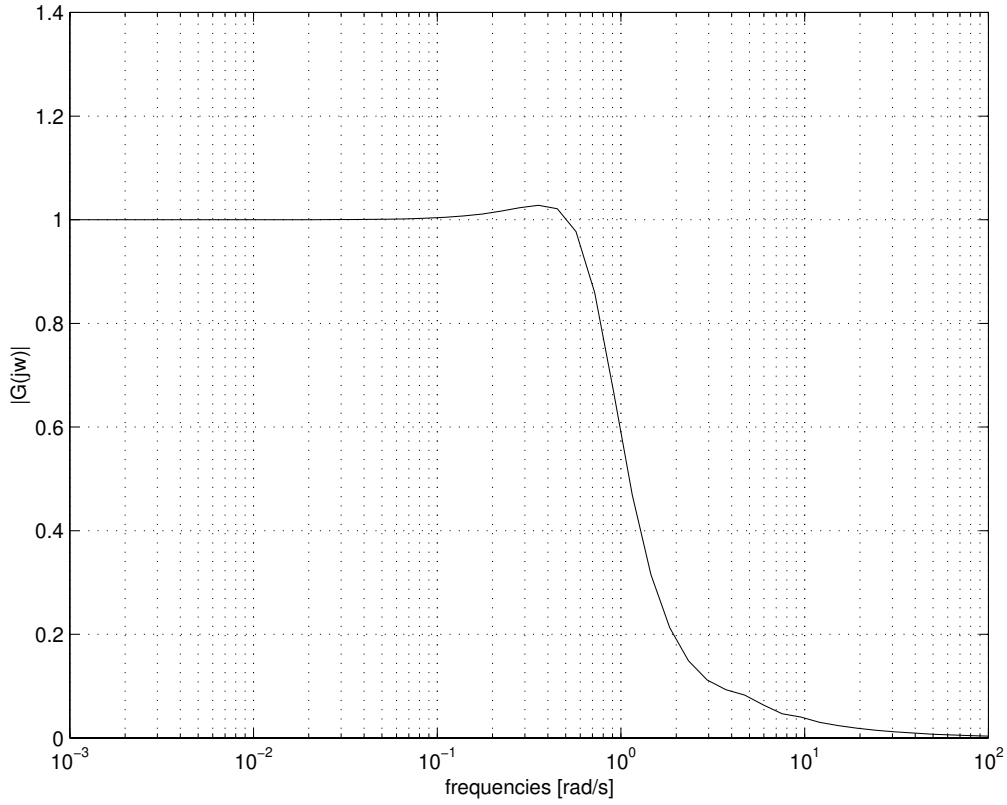

(c)

Figure 2: Pipes linear car following model: (a) Impulse response $g_p(t)$ vs t (b) $\int_0^t |g_p(\tau)|d\tau$ vs t and (c) $|G_p(j\omega)|$ vs ω.

parameters by fitting real traffic data. The following parameter values were used in the optimal control model

$$C_S = 1.64s^{-2}$$
$$C_C = 1.14s$$
$$C_V = 0.5s^{-1}$$

The vehicle dynamics are modeled as

$$\dot{v}_F = u(t-\tau) - \rho v_F - \beta v_F^2 \tag{14}$$

where ρ : mechanical drag coefficient (about 10^{-3} to 10^{-2} $\sec^{-1}$)
β : aerodynamic drag coefficient (about 10^{-5} to 10^{-4} m^{-1})

The response of the model to an impulse function does not change sign for $t > 0$ (fig 3(a)), implying that the optimal control model has a smooth response devoid of any oscillations. However, to ascertain string stability by theorem 1, we require the impulse response of a linear system. Hence we need to linearize (14) and obtain the transfer function that relates the velocity of the leading vehicle to that of the following vehicle. However, the point of equilibrium about which the linearization is to be performed depends on the operating speed of the vehicle, which in turn depends on the speed of the leading vehicle. To account for this we perform linearization at equilibrium speeds of 0m/s, 15m/s and 25m/s. Equation (14) can be written as

$$\dot{v}_F = u(t-\tau) - Av_F \tag{15}$$

where A depends on the speed around which the linearization is done. The values of A for the different equilibrium speeds are given as (for $\rho = 0.005s^{-1}$ and $\beta = 0.00025m^{-1}$)

$$A = \begin{cases} 0.005s^{-1} & 0m/s \\ 0.0125s^{-1} & 15m/s \\ 0.0175s^{-1} & 25m/s \end{cases}$$

Using (13) and (15) for the listed parameter values, we get the transfer function of the linearized model as

$$G_o(s) = \frac{v_i}{v_{i-1}} = \frac{(0.5s + 1.64)e^{-0.09s}}{s^2 + As + (2.3696s + 1.64)e^{-0.09s}} \tag{16}$$

We find that for the different values of A, the impulse response and the magnitude $|G_o(j\omega)|$ is negligibly different. A takes small values for the different operating speeds that differ by the order of 10^{-3}. When this numerical value is combined with the rest and

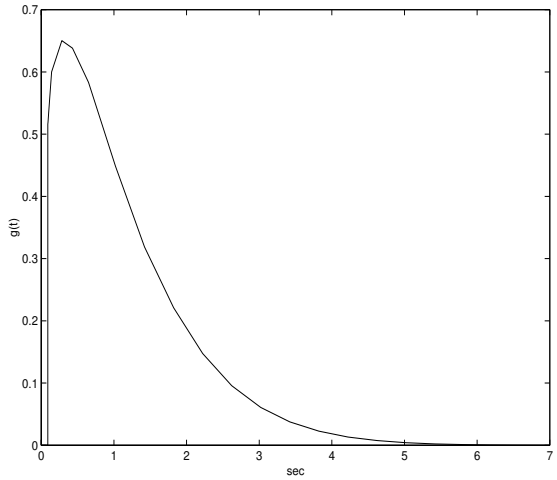

(a)

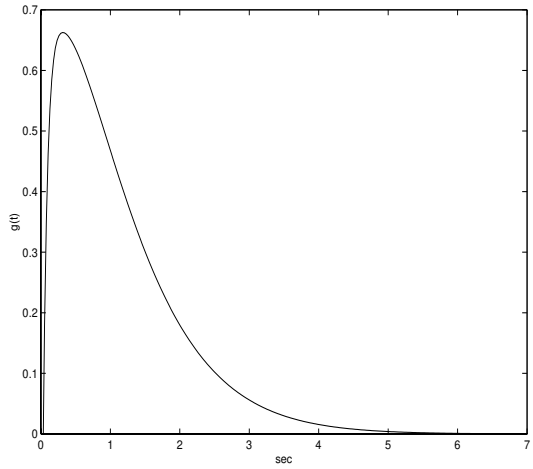

(b)

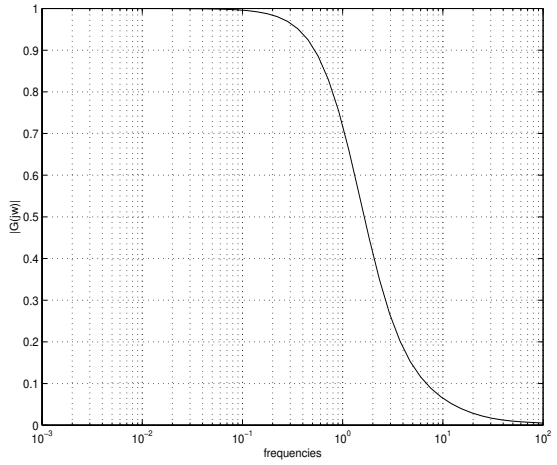

(c)

Figure 3: Optimal control car following model: (a) Response of the nonlinear model to an impulse function, (b) impulse response $g_o(t)$ vs t and (c) $|G_o(j\omega)|$ vs ω when the model is linearized around the operating speed of 15m/s.

the impulse response calculated, the difference is negligible. Figure 3(b)-(c) plots the impulse response and $|G_o(j\omega)|$ for an operating speed of 15m/s, respectively. We observe that the impulse response $g_o(t)$ does not change sign for $t > 0$ and satisfies (6), i.e. $\|g_o\|_1 = 1$. Also $|G_o(j\omega)|$ is less than unity for all $\omega > 0$. From the analysis we can conclude that the optimal control model belongs to the class of systems that guarantee string stability.

Look Ahead Model

This model [11,12] is based on the hypotheses that the human driver observes the behavior of three vehicles directly ahead. It incorporates a switching logic that determines whether to follow the velocity of the first or the second lead vehicle. The switching logic determines the majority direction of acceleration and then actuates the mode switch accordingly. This simple model has two different transfer functions, depending on the two positions of the switch. The gains are given by

$$G_{l1}(s) = \frac{v_i}{v_{i-1}} = \frac{0.2}{s + 0.2} \qquad \text{(position 1)} \qquad \text{(17a)}$$

$$G_{l2}(s) = \frac{v_i}{v_{i-1}} = \frac{0.65}{s + 0.65} \qquad \text{(position 2)} \qquad \text{(17b)}$$

From (17) we have that the impulse responses are given by

$$g_{l1}(t) = 0.2e^{-0.2t} \text{ and } g_{l2}(t) = 0.65e^{-0.65t}$$

$$\Rightarrow \|g\|_1 = 1$$

Moreover, $g(t) > 0$ for all $t>0$. Figure 4 shows the impulse response, $\int_0^t |g_{l1}(\tau)| d\tau$ and $|G_{l1}(j\omega)|$ for 17(a).

It follows that the look ahead model belongs to the class of systems that guarantee string stability. The magnitude $|G(j\omega)|$ is less than unity for all $\omega > 0$ for both positions of the switch in the model.

2.3 String Stability of Semi-Automated Vehicles

We now consider the string stability of a fleet of semi-automated vehicles closely following each other in a single lane. The ICC model given in [1] is used to represent the semi-automated vehicles. For longitudinal control, the automatic control system of the semi-automated vehicle may be considered as having two input variables: throttle angle command and brake command, and one output variable: vehicle speed [1]. The other inputs such as aerodynamic drag, road conditions and vehicle mass changes are treated as

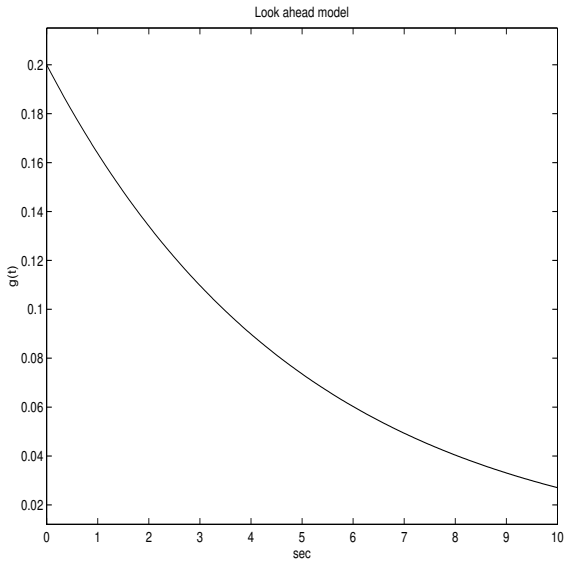

(a)

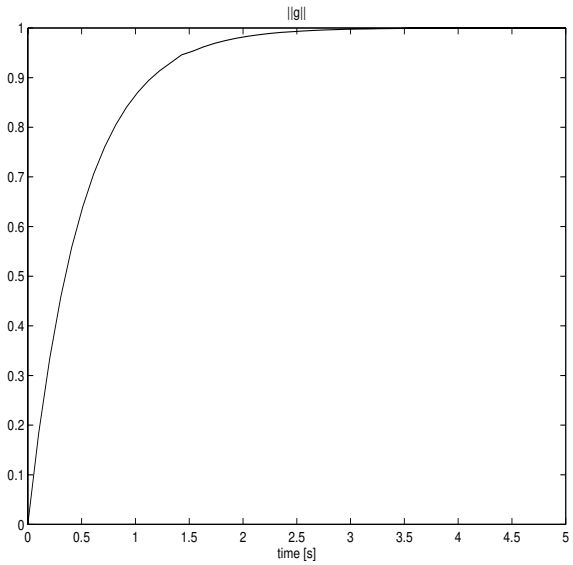

(b)

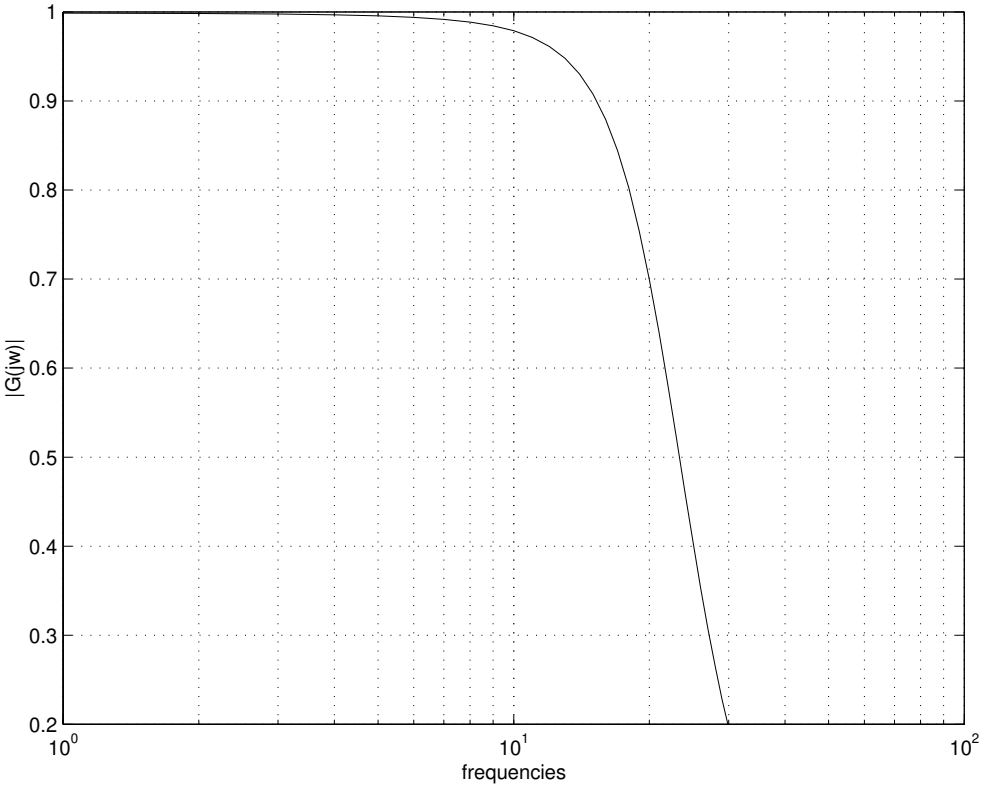

(c)

Figure 4: Look ahead car following model: (a) Impulse response $g_{l1}(t)$ vs t (b) $\int_0^t |g_{l1}(\tau)|d\tau$ vs t and (c) $|G_{l1}(j\omega)|$ vs ω.

disturbances. The semi-automated vehicle is assumed to have a constant time headway policy. We consider the throttle and the brake subsystems separately, as they are not allowed to act simultaneously.

Throttle Controller

The closed loop transfer function for the throttle subsystem is given by [1]

$$G_{th}(s) = \frac{\delta_i}{\delta_{i-1}} = \frac{(a + bk_1)s^2 + b(k_2 + k_3)s + bk_4}{s^3 + (a + bk_1 + bk_2h)s^2 + b(k_2 + k_3 + k_4h)s + bk_4} \quad (18)$$

where k_1, k_2, k_3, k_4: designed controller parameters
h: time headway desired
a, b: coefficients determined by the operating point which is the speed of the vehicle ahead

It is important to note that the time headway defined in this paper is the time taken by the vehicle to cover the intervehicle distance measured from the rear of the preceding vehicle to the rear of the following vehicle. The throttle controller is designed to control the throttle angle of the semi-automated vehicle using the design controller parameters k_1 to k_4 that are chosen using a pole placement as follows [1]:

$$\begin{aligned} k_1 &= (\lambda_0 + 2\zeta\omega_n - bk_2h - a)/b \\ k_2 &= 0.2/b \\ k_3 &= (2\zeta\omega_n\lambda_0 + \omega_n^2 - bk_2 - h\lambda_0\omega_n^2)/b \\ k_4 &= \lambda_0\omega_n^2/b \end{aligned} \quad (19)$$

where λ_0: desired pole
ω_n, ζ: natural frequency and damping ratio of the two desired complex poles, respectively.

The throttle controller in (18) is applied to a validated nonlinear vehicle model and tested through a series of simulations with the following parameter values that satisfy the performance criteria [1]

$\lambda_0 = 1.2$, $\omega_n = 0.1$, $\zeta = 1$ and a constant time headway *h*=1 sec.

Using these values in (19) to get the design parameter values and substituting them in (18) we obtain

$$G_{th}(s) = \frac{1.2s^2 + 0.24s + 0.012}{s^3 + 1.4s^2 + 0.25s + 0.012} \quad (20)$$

The L_1 norm of the throttle subsystem (20) is

$$\|g_{th}\|_1 = 1$$

Also the impulse response $g_{th}(t) > 0$ for all $t>0$ (fig 5). Thus, the throttle controller of the semi-automated vehicle belongs to the class of systems that guarantee string stability. Moreover, $|G_{th}(j\omega)|$ is less than unity for all $\omega > 0$.

Human factor considerations dictate that the response of a semi-automated vehicle should be smooth. Therefore, there are two constraints imposed on the throttle controller due to smooth ride requirement [1]. The constraints are the following:

C-I: $a_{\min} \le \dot{V}_f \le a_{\max}$ where $a_{\min}$ and $a_{\max}$ are specified.

C-II: The absolute value of the jerk defined as $\ddot{V}_f$ should be as small as possible.

The controller in (20) does not guarantee that the above two constraints will always be satisfied. For example, if the lead vehicle rapidly changes its velocity at a particular point, it may create a large relative velocity error and spacing error, which in turn may cause large throttle angle and acceleration, violating C-I and C-II. Also there may be large initial position and velocity errors when the following vehicle switches from one leading vehicle to another due to lane change, merging etc., leading to high acceleration/deceleration that may violate C-I, C-II. In order to avoid these occurrences, two limiters are used in the throttle controller of [1].

The first is an acceleration limiter to protect the semi-automated vehicle from responding to erratic behavior of the leading vehicle. The velocity of the leading vehicle V_l is passed through an acceleration limiter shown in fig 6 where p is some positive constant. Instead of following V_l the throttle controller is designed to follow $\hat{V}_l$. The acceleration limiter limits the maximum and minimum acceleration of the target velocity to $a_{\max}$ and $a_{\min}$, respectively. It eliminates any sudden changes in V_l during transients and presents a smooth target velocity for the controller to follow. At steady state, $\hat{V}_l$ approaches V_l, therefore following the former the throttle controller will eventually reach V_l in a smooth way.

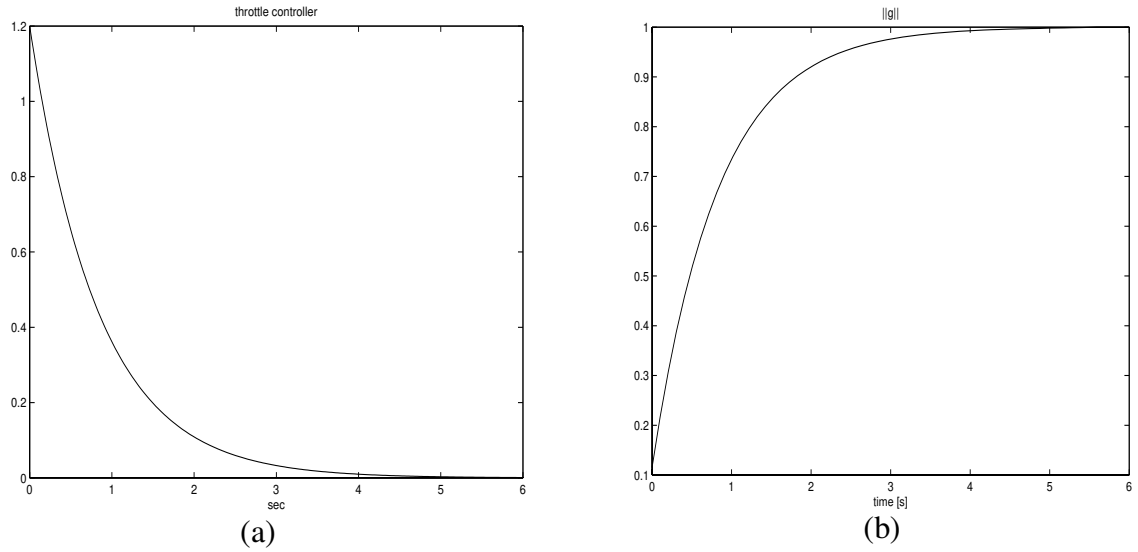

(a) (b)

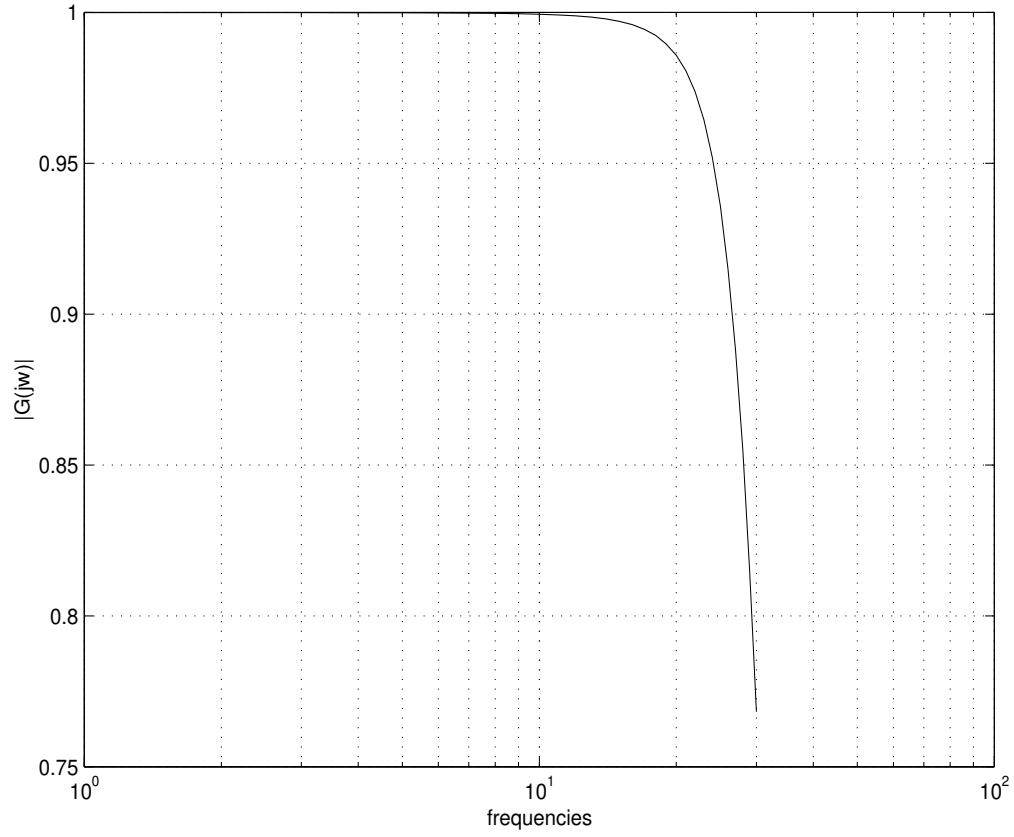

(c)

Figure 5: Throttle controller subsystem: (a) Impulse response $g_{th}(t)$ vs t (b) $\int_0^t |g_{th}(\tau)| d\tau$ vs t and (c) $|G_{th}(j\omega)|$ vs ω.

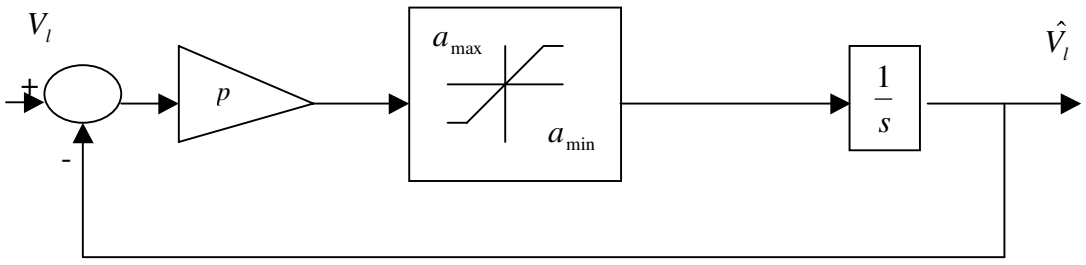

Figure 6: Acceleration Limiter.

In 100% semi-automated traffic, the acceleration limiter will not affect string stability since all vehicles (with the exception of emergency stopping) are assumed to operate within the limits of $a_{\max}$ and $a_{\min}$. In mixed traffic this may not be the case because the manually driven vehicles may generate trajectories outside the desired acceleration limits.

In addition to the acceleration limiter, the spacing error is passed through a saturation element to take care of large spacing errors being fed into the controller. The saturation element $sat(\delta)$ is defined as

$$sat(\delta) = \begin{cases} e_{\max} & if \quad \delta > e_{\max} \\ e_{\min} & if \quad \delta < e_{\min} \\ \delta & otherwise \end{cases}$$

This prevents any large spacing error and limits the spacing error measurements seen by the throttle controller to be within $e_{\max}$ and $e_{\min}$. In other ICC designs similar modifications are used to maintain smooth response.

Brake Controller

For the closed loop brake subsystem we have the following transfer function [1]

$$G_{br}(s) = \frac{v_i}{v_{i-1}} = \frac{k_5 s + k_6}{s^2 + (k_5 + k_6 h)s + k_6} \tag{21}$$

where k_5, k_6: brake controller gains
h: time headway desired

Equation (21) is investigated for $h = 1s$ with the following gains that satisfy the performance criteria given in [1]

$$k_5 = 1$$
$$k_6 = 0.25$$

From the impulse response of (21) we have

$$\| g_{br} \|_1 = 1$$

and $g_{br}(t) > 0$ for all $t > 0$ (fig 7) implying that the brake controller does not have an oscillatory response. Hence, like the throttle controller, the brake controller also belongs to the class of systems that guarantee string stability. Furthermore, $|G_{br}(j\omega)|$ is less than unity for all $\omega > 0$.

Therefore, we have shown that both the throttle and the brake subsystems belong to the class of systems that guarantee string stability provided that they remain within the saturation limits used. It is important to note that the design parameters of the controllers can be modified such that the throttle and the brake controller subsystems may violate (6) and not belong to the class of systems that guarantee string stability.

2.4 String Stability of Mixed Vehicles

The mixed traffic system consists of manual and semi-automated vehicles whose dynamics are given by the models presented in the previous sections. Consider the manual vehicles to be represented by the Pipes model, which does not belong to the class of systems that guarantee string stability and may generate slinky-type effects. Therefore, we cannot guarantee string stability for the system of mixed vehicles.

However, as stated before, definition 1 of string stability is conservative. Though the string of mixed vehicles may not be string stable, the behavior of the whole system may be acceptable. We carry out an analysis that should provide some insight into the dynamics of mixed traffic during transients. Consider vehicle following transients for two different cases:

(i) Lead manual vehicle in mixed traffic performs a smooth acceleration maneuver.

(ii) Lead manual vehicle in mixed traffic performs a rapid acceleration maneuver.

(i) Lead manual vehicle in mixed traffic performs a smooth acceleration maneuver

Using the ICC model presented in the previous section to represent semi-automated vehicles, a smooth acceleration maneuver by lead manual vehicle means that the target speed is within the saturation limits of the ICC acceleration limiter. Considering mixing

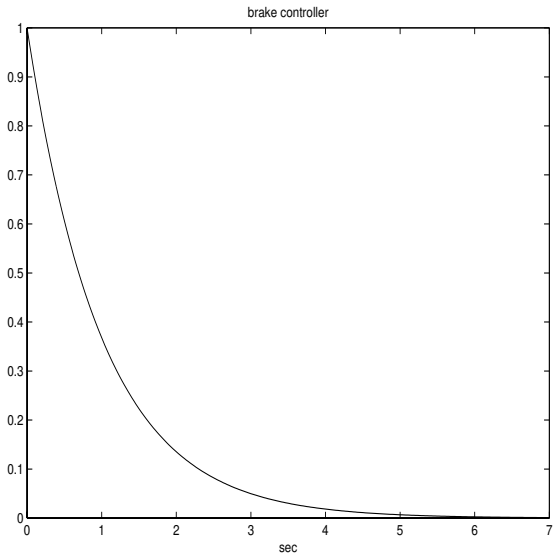

(a)

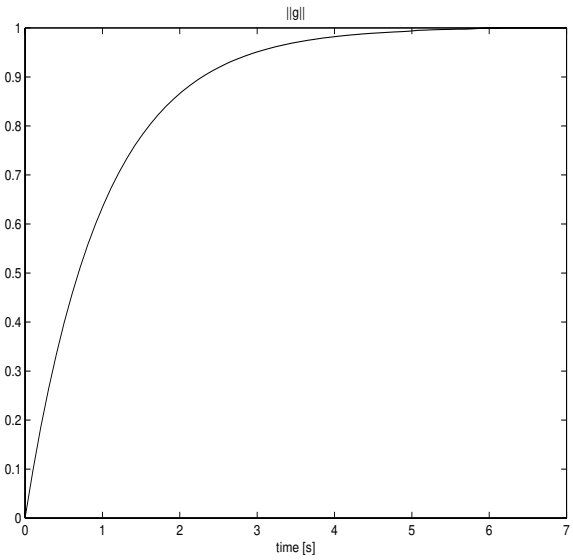

(b)

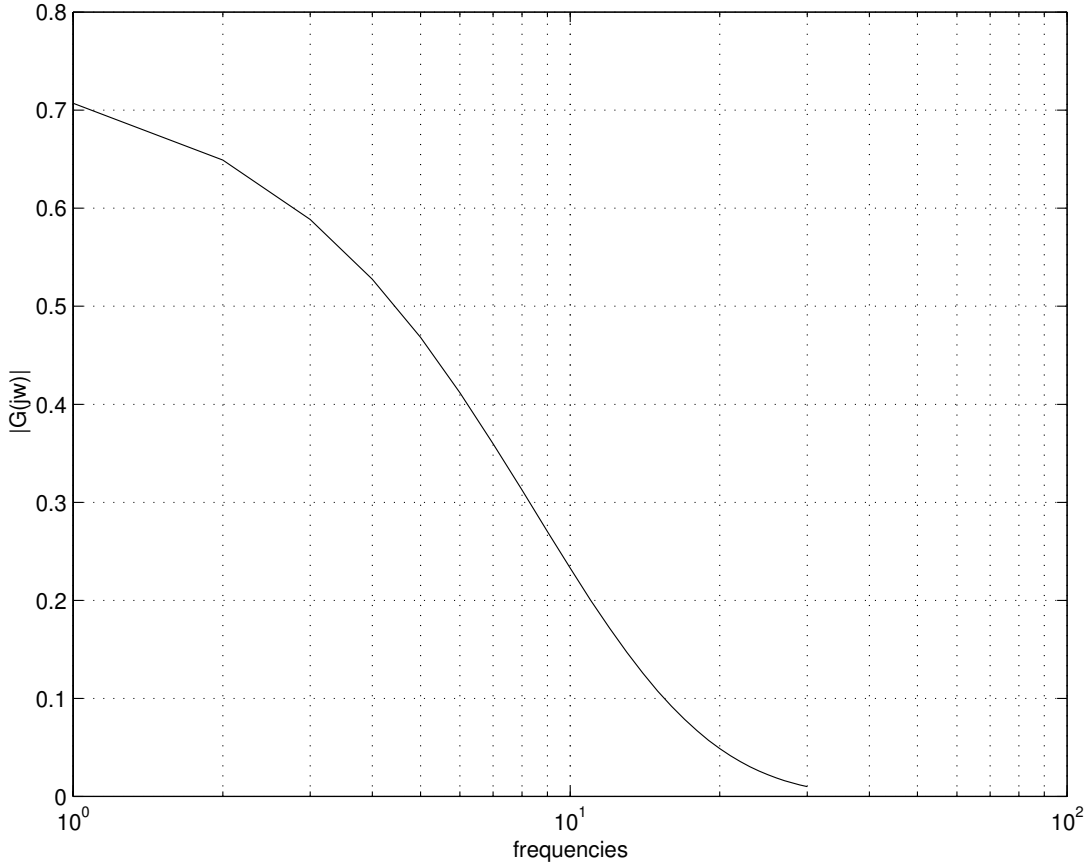

(c)

Figure 7: Brake controller subsystem: (a) Impulse response $g_{br}(t)$ vs t (b) $\int_0^t |g_{br}(\tau)|d\tau$ vs t and (c) $|G_{br}(j\omega)|$ vs ω.

of vehicles of different classes, we get the error propagation transfer functions as (from (4) and (5))

$$\frac{\delta_i}{\delta_{i-1}} = \frac{1 - G_i - sh_i G_i}{1 - G_{i-1} - sh_{i-1} G_{i-1}} G_{i-1} = G_{ii-1}(s) \tag{22}$$

$$\frac{v_{ri}}{v_{ri-1}} = \frac{a_{ri}}{a_{ri-1}} = \frac{(1 - G_i)}{(1 - G_{i-1})} G_{i-1} = \overline{G_i}(s) \tag{23}$$

Examining (22) we can conclude that given $G_i(s)$ there may exist a h_i э $1 - G_i(s) - sh_i G_i(s) = 0 \ \forall s$. The existence of such h_i is given by the following lemma.

Lemma 3: A constant h_i exists for a given $G_i(s) = \frac{n(s)}{d(s)}$ such that $1 - G_i(s) - sh_i G_i(s) = 0 \ \forall s$ if and only if degree ($d(s)$)-degree ($n(s)$)=1 and for $d(s) = s^n + a_1 s^{n-1} + \ldots\ldots + a_{n-1} s + a_n$ and $n(s) = b_1 s^{n-1} + b_2 s^{n-2} + \ldots\ldots + b_{n-1} s + b_n$, where a_1, $a_2, \ldots, a_n$, b_1, $b_2, \ldots, b_n$ are constants with $a_n = b_n$, the following is true

$$\frac{b_{n-1}}{a_{n-1} b_1 - b_n} = \ldots\ldots = \frac{b_1}{a_1 b_1 - b_2} = \frac{1}{b_1} = h > 0 \tag{24}$$

where $h_i = h$.

The proof is simple and omitted.

✧

The existence of h_i to satisfy lemma 3 exactly is a singular case. The use of h_i however, guarantees that the following vehicle will maintain zero position, velocity and acceleration errors during vehicle following. In other words, with h_i the two vehicles, lead and following will be electronically connected and behave as a single vehicle. Choosing h_i to satisfy lemma 3 is not practical. However, choosing a time headway close to h_i is possible leading to tight vehicle following. This is demonstrated in the following example:

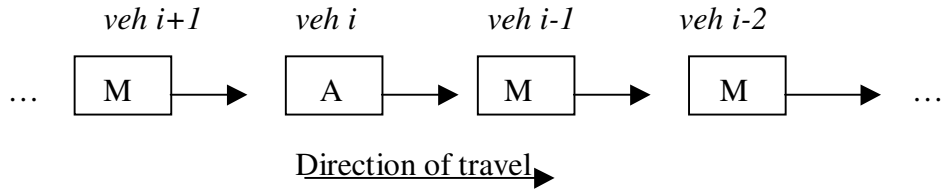

A: semi-automated vehicle
M: manual vehicle

Figure 8: Mixed manual/semi-automated traffic.

Consider a string of mixed manual/semi-automated vehicles as depicted in fig 8. Vehicle *i* is a semi-automated vehicle while vehicle *i-1* and the rest are manual vehicles. All vehicles are assumed to follow a constant time headway policy.

We choose Pipes model [8,9] to represent manually driven vehicles since this is the only human driver car following model that models the slinky-type effects we observe in today's traffic. We later demonstrate this in section 2.5 using simulations. We assume that the semi-automated vehicles follow a time headway of 1.0s and the manual vehicles follow a time headway of 1.8s, which is taken as the "national average" for manual traffic [16]. Therefore, we have

$$\frac{\delta_i}{\delta_{i-1}} = \frac{1 - G_{th} - sG_{th}}{1 - G_p - 1.8sG_p} G_p = G_{ii-1}(s) \tag{26}$$

where $G_p(s)$ is taken from (12) and $G_{th}(s)$ is the transfer function of the ICC vehicle. The time delay is approximated using

$$e^{-Ts} \approx \frac{1}{1+Ts}$$

to obtain

$$G_p(s) = \frac{0.37}{1.5s^2 + s + 0.37}$$

and from (20)

$$G_{th}(s) = \frac{1.2s^2 + 0.24s + 0.012}{s^3 + 1.4s^2 + 0.25s + 0.012}$$

So after substituting for $G_p(s)$ and $G_{th}(s)$ in (26) and rearranging the terms, we have

$$\frac{\delta_i}{\delta_{i-1}} = -\frac{0.074s^3 + 0.014s^2 + .0007s}{1.5s^5 + 2.434s^4 + 0.8426s^3 + 0.1015s^2 + 0.004s} = G_{ii-1}(s)$$

The gain of the velocity and the acceleration errors is given by (24)

$$\frac{v_{ri}}{v_{ri-1}} = \frac{a_{ri}}{a_{ri-1}} = \frac{(1 - G_i)}{(1 - G_{i-1})} G_{i-1} = \overline{G_i}(s)$$

where

$$\overline{G_i} = \frac{(1 - G_{th})}{(1 - G_p)} G_p = \frac{0.37s^3 + 0.074s^2 + .0037s}{1.5s^5 + 3.1s^4 + 1.775s^3 + 0.268s^2 + 0.012s} = \tilde{G}_{ii-1}(s)$$

Calculating the impulse responses of the above two error systems, we get

$$g_{ii-1}(t) = 0.051e^{-1.12t} - 0.05e^{-0.222t} - 0.016e^{-0.107t} + 0.014e^{-0.094t}$$

and

$$\tilde{g}_{ii-1}(t) = -0.463e^{-1.2t} + 0.463e^{-0.667t}$$

We find that $\|g_{ii-1}\|_1 = 0.175$ and $\|\tilde{g}_{ii-1}\|_1 = 0.308$ which shows that the semi-automated vehicle attenuates the position, velocity and acceleration errors and does not contribute to the slinky effect phenomenon. On the other hand, if vehicle *i* were a manually driven vehicle as in manual traffic, the error propagation would be given by $\|g_p\|_1 = 1.1$ as shown in section 2.2, from which we could not exclude the possibility of error amplification or the existence of slinky-type effects.

We can verify from (26) that the impulse response $g_{ii-1}(t)$ of $G_{ii-1}(s)$ depends on the headways of manual and semi-automated vehicles. It is possible to have manual vehicles follow headways other than the mean value of 1.8s. Also some semi-automated vehicles may be programmed to use headways other than 1.0s. To carry out the above analysis under such varied situations, we can use the plots in fig 9. The area under the curve of $g_{ii-1}(t)$ is plotted in fig 9(a) as a function of the semi-automated vehicle headway from 0.5s to 1.5s for different manual vehicle headway of 1.0s, 1.8s and 2.2s, and is a linear function of h_i, the semi-automated vehicle headway. The $\|g_{ii-1}\|_1$ is plotted in fig 9(b) while fig 9(c) plots $\|g_{ii-1}\|_1$ as a function of manual vehicle headway from 0.7s to 2.2s for different semi-automated vehicle headway of 0.5s, 1.0s and 1.5s. Using lemma 3 we can show that for *h*=1/1.2 we have $\|g_{ii-1}\|_1$=0 as seen in fig 9(b).

To analyze the effect of error attenuation by a semi-automated vehicle on the following vehicle, let us consider the position, velocity and acceleration errors for manual vehicle *i+1*. We have

$$\frac{\delta_{i+1}}{\delta_i} = \frac{1 - G_p - 1.8sG_p}{1 - G_{th} - sG_{th}} G_{th}$$

$$= -\frac{1.8s^4 + 0.7608s^3 + 0.0982s^2 + 0.004s}{0.3s^5 + 0.26s^4 + 0.117s^3 + 0.0168s^2 + 0.0007s} = G_{ii+1}$$

and

$$\frac{v_{ri+1}}{v_{ri}} = \frac{a_{ri+1}}{a_{ri}} = \frac{(1 - G_p)}{(1 - G_{th})} G_{th}$$

$$= \frac{1.8s^4 + 1.56s^3 + 0.258s^2 + 0.012s}{1.5s^5 + 1.3s^4 + 0.585s^3 + 0.084s^2 + 0.0037s} = \tilde{G}_{ii+1}$$

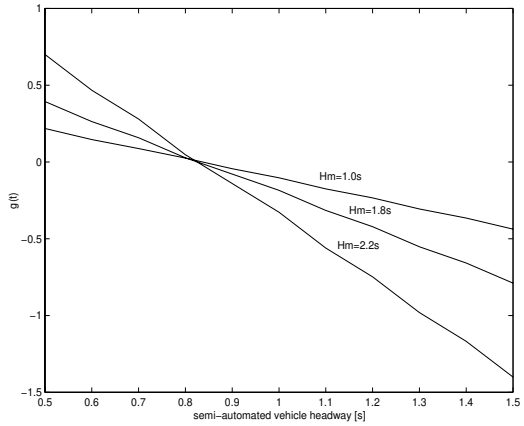

Figure 9(a): Area under the curve of $g_{ii-1}(t)$ as a function of semi-automated vehicle headway from 0.5s to 1.5s for different manual vehicle headways of 1.0s, 1.8s and 2.2s.

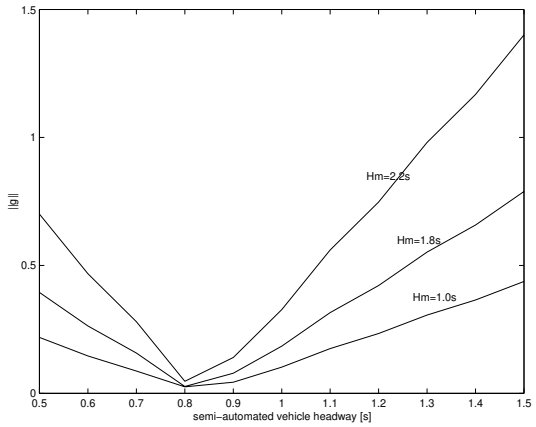

Figure 9(b): $\|g_{ii-1}\|_1$ as a function of semi-automated vehicle headway from 0.5s to 1.5s for different manual vehicle headways of 1.0s, 1.8s and 2.2s.

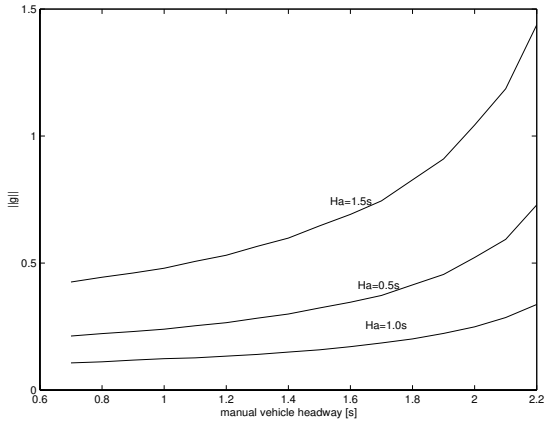

Figure 9(c): $\|g_{ii-1}\|_1$ as a function of manual vehicle headway from 0.6s to 2.2s for different semi-automated vehicle headways of 0.5s, 1.0s and 1.5s.

The impulse responses are given by

$$g_{ii+1}(t) = -5.99e^{-0.333t}\cos(0.369t) + 1.829e^{-0.333t}\sin(0.369t) + 0.041e^{-0.127t} - 0.051e^{-0.074t}$$

$$\tilde{g}_{ii+1}(t) = 1.2e^{-0.333t}\cos(0.368t) + 1.086e^{-0.333t}\sin(0.368t)$$

We obtain $\|g_{ii+1}\|_1 = 11.78$ and $\|\tilde{g}_{ii+1}\|_1 = 3.88$ which shows that the manual vehicle following the semi-automated vehicle may amplify the position, velocity and acceleration errors. So no conclusion is possible for the tracking errors of vehicle *i+1* from the above analysis.

(ii) Lead manual vehicle in mixed traffic performs a rapid acceleration maneuver

Using the ICC model for semi-automated vehicles, a rapid acceleration maneuver by lead manual vehicle means acceleration at a rate greater than $a_{\max}$. In such circumstances we later demonstrate that the semi-automated vehicle improves traffic flow characteristics. It filters the response of the rapidly accelerating lead manual vehicle in an effort to maintain smooth driving. This is done at the expense of larger position, velocity and acceleration errors and sometimes at the expense of falling far behind the vehicle ahead. This smoothing of traffic flow by the semi-automated vehicle is beneficial for the environment, as we shall observe in section 3.

2.5 Simulations

Manual Traffic

We examine the vehicle following transients in dense manual traffic where a string of 10 manually driven vehicles follow a lead vehicle in a single lane without passing. The Pipes linear car following model is used to model the manual vehicles. The lead vehicle accelerates from 0m/s to 20m/s with an acceleration of about 0.075g and the rest of the vehicles follow suit. Figure 10(a) shows the onset of slinky-type effect in the velocity responses of the following vehicles. We also observe in fig 10(b) that the position errors are amplified as they propagate upstream. The simulation results demonstrate that a string of vehicles represented by Pipes car following model exhibits string instability.

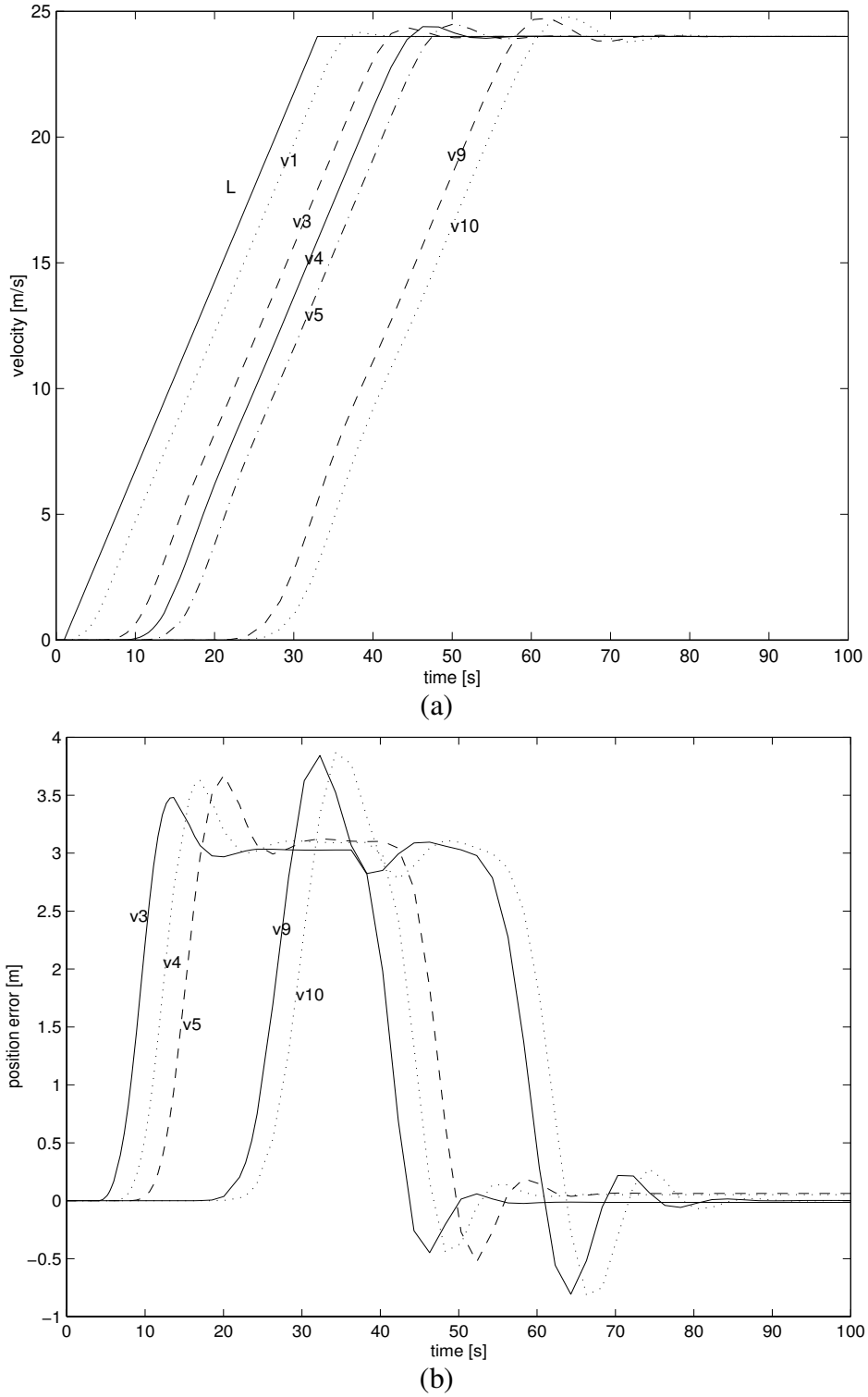

Figure 10: 10 vehicles in manual traffic (Pipes model) following a lead vehicle. (a) Velocity response of leader (L), 1st vehicle (v1) and vehicles 3 to 5 (v3-v5) and 9,10 (v9, v10); (b) position error of vehicles 3 to 5 (v3-v5) and 9,10 (v9, v10).

Mixed Traffic

We now consider a string of 10 vehicles in mixed manual/semi-automated traffic. We demonstrated above that the Pipes model models the slinky-type effects we observe in today's manual traffic. Therefore we use the Pipes model to examine the effect of mixing semi-automated and manually driven vehicles on the traffic flow characteristics during transients. The ICC model presented in section 2.3 is used to simulate semi-automated vehicles. Assume the 4^{th} vehicle to be semi-automated which corresponds to 10% mixing of semi-automated with manual vehicles. Consider two separate cases:

(i) Smooth acceleration by lead vehicle.

(ii) Rapid acceleration by lead vehicle.

(i) Smooth acceleration by lead vehicle

The lead vehicle accelerates smoothly from 0m/s to 20m/s at 0.075g and the rest follow suit. The velocity responses in fig 11(a) show good tracking by the semi-automated vehicle v4. It attenuates the position error and does not contribute to the slinky effect phenomenon as shown in fig 11(b).

(ii) Rapid acceleration by lead vehicle

The lead vehicle accelerates at 0.35g from 0m/s to 24.5m/s, maintains a constant speed at 24.5m/s, thereafter decelerates to 14.5m/s at 0.3g and finally accelerates to 24.5m/s at 0.25g. The acceleration and deceleration values used are typical for many passenger cars [4]. The velocity responses in fig 12(a) show that the semi-automated vehicle v4 filters the response of the rapidly accelerating vehicle v3 in an effort to maintain smooth driving. As a result the responses of vehicles v5, v9 and v10 are less oscillatory than that of v1 and v3. However, this is done at the expense of large position error in v4 (fig 12(b)).

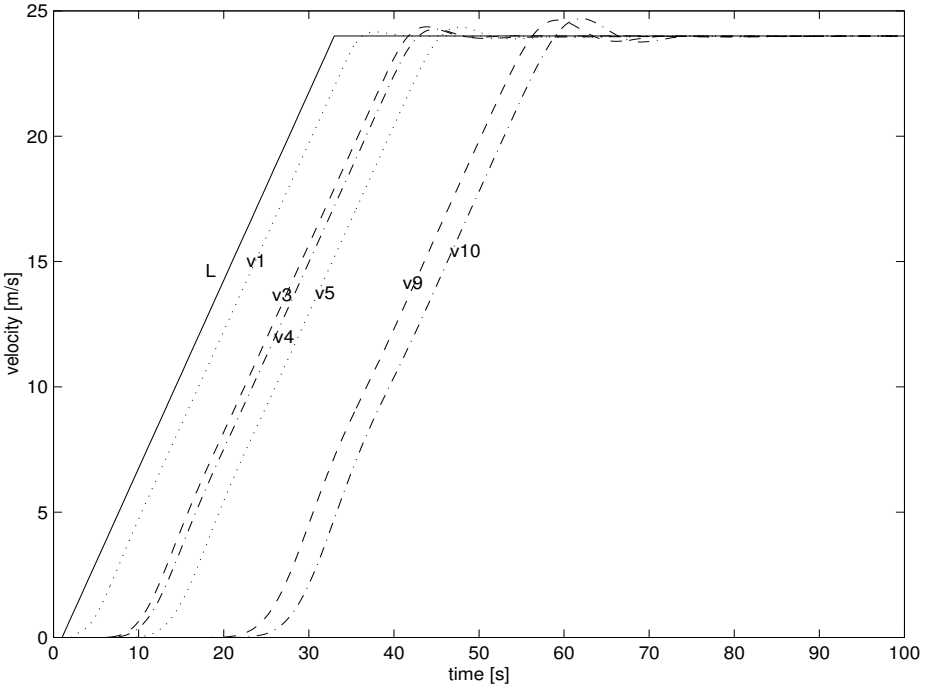

(a)

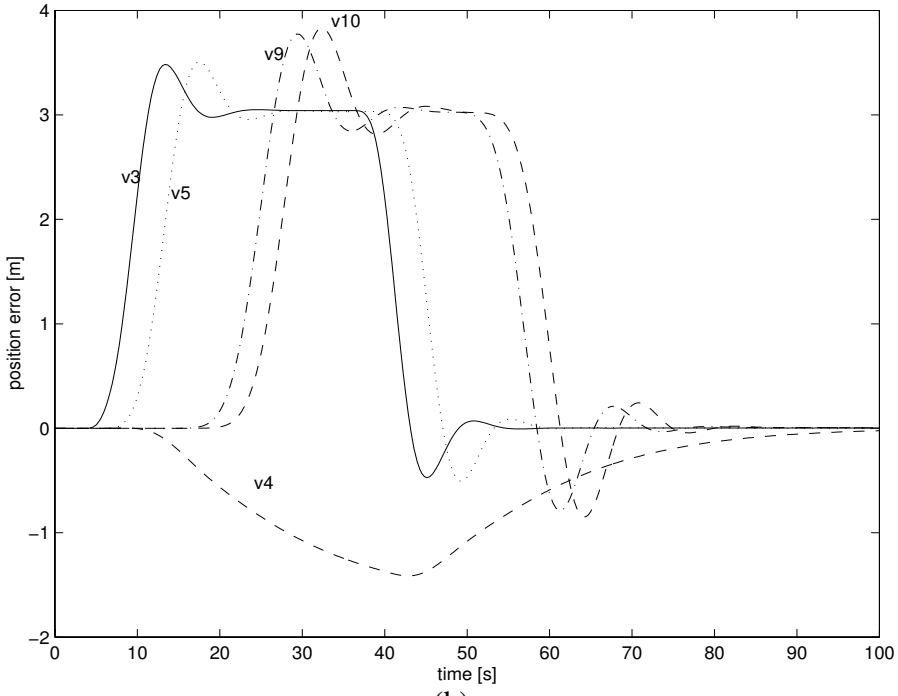

(b)

Figure 11: 10 vehicles in mixed manual (Pipes model)/semi-automated traffic following a lead vehicle performing smooth acceleration maneuvers. The 4th vehicle (v4) is semi-automated.(a) Velocity response of leader (L), 1st vehicle (v1) and vehicles 3 to 5 (v3-v5) and 9,10 (v9, v10); (b) position error of vehicles 3 to 5 (v3-v5) and 9,10 (v9, v10).

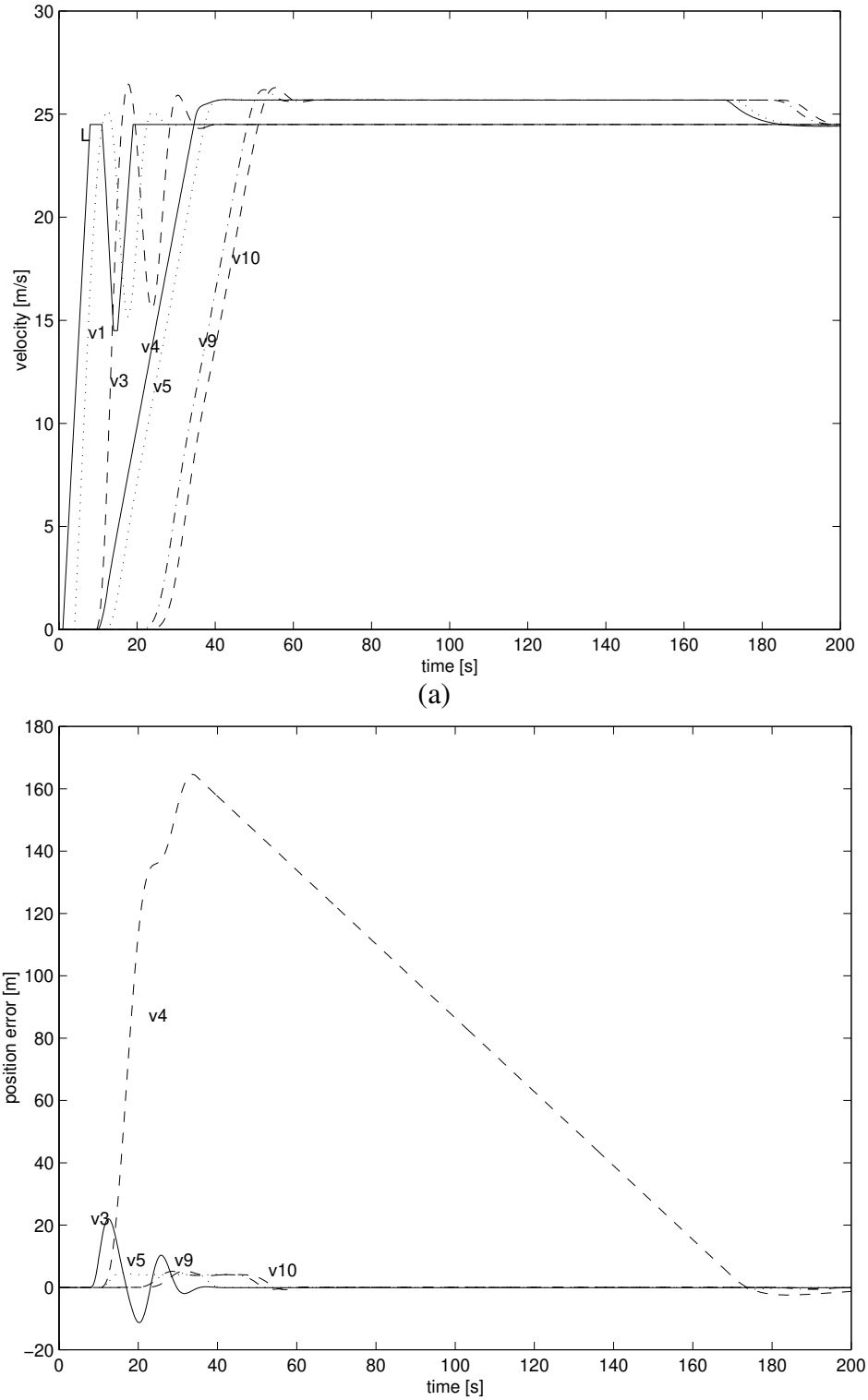

Figure 12: 10 vehicles in mixed manual (Pipes model)/semi-automated traffic following a rapidly accelerating lead vehicle. The 4th vehicle (v4) is semi-automated. (a) Velocity response of leader (L), 1st vehicle (v1) and vehicles 3 to 5 (v3-v5) and 9,10 (v9, v10); (b) position error of vehicles 3 to 5 (v3-v5) and 9,10 (v9, v10).

3 Environmental Impact of Mixed Traffic

3.1 Introduction

In this section we explore the benefits of semi-automated vehicles in mixed traffic in terms of pollution and fuel consumption. For traffic simulation models at the microscopic level, vehicle parameters such as second-by-second velocity, acceleration and grade for each individual vehicle determines the emission levels and fuel consumption [14]. For our simulation, we assume that the vehicles travel in a flat road with no change in grade and no wind gust. Secondary variables such as accessories like air-conditioning are neglected.

The technique we employ is to use velocity/acceleration look-up tables of emission and fuel consumption values and integrate them with our simulation of manual/mixed traffic. The quantities measured are the tailpipe emissions of unburnt hydrocarbons (HC), carbon monoxide (CO), oxides of nitrogen (NO, NO_2, denoted by NO_x in this paper) and fuel consumption. The maps are the ones used by the Federal Highway Administration (FHWA) for their TRAF models [13]. They were created in 1986 and though they are somewhat out of date, they are pretty much the public domain ones currently in use. We plot the different look-up tables for CO, NO_x, HC emissions and fuel consumption values in fig 13. They are indexed by speed and acceleration. The speed increments are from 0 to 70 ft/s while the acceleration increments are from –9 to +9 ft/s^2. The units for emission and fuel are mg/second and 10^{-5} gallons/second, respectively.

3.2 Simulations

We examine the possible environmental benefits due to the presence of semi-automated vehicles in mixed traffic using the simulations in section 2.5 for a string of 10 vehicles following a lead vehicle. When the lead vehicle performs smooth acceleration maneuvers, there are no significant differences in pollution emission and fuel consumption between manual traffic (fig 10) and mixed traffic (fig 11).

When the lead manual vehicle performs rapid acceleration maneuvers as in fig 12, the pollution emissions and fuel consumption in manual traffic can be considerably reduced due to the presence of the semi-automated vehicle. Figure 14 shows the velocity responses of 6 vehicles in a string of 10 manually driven vehicles following a lead vehicle performing rapid acceleration maneuvers as in fig 12. The total CO, NO_x and HC emissions and fuel consumption by manual traffic (fig 14) are compared with that of mixed traffic (fig 12) in fig 15. The smoothing of traffic flow by the semi-automated vehicle significantly improves pollution levels and fuel consumption of manual traffic as indicated in table 1.

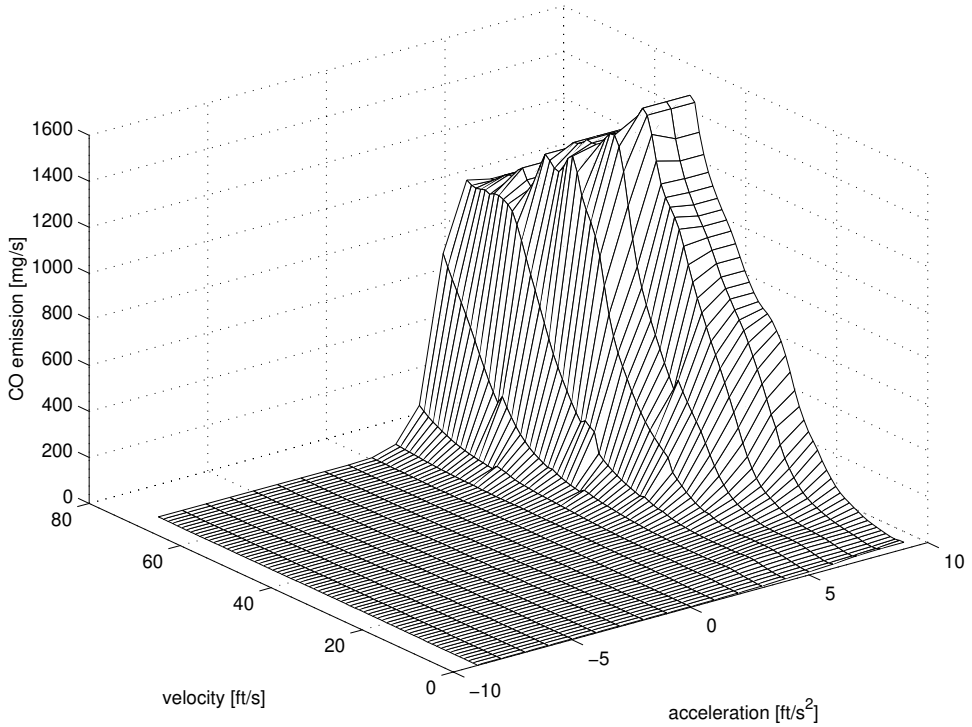

(a)

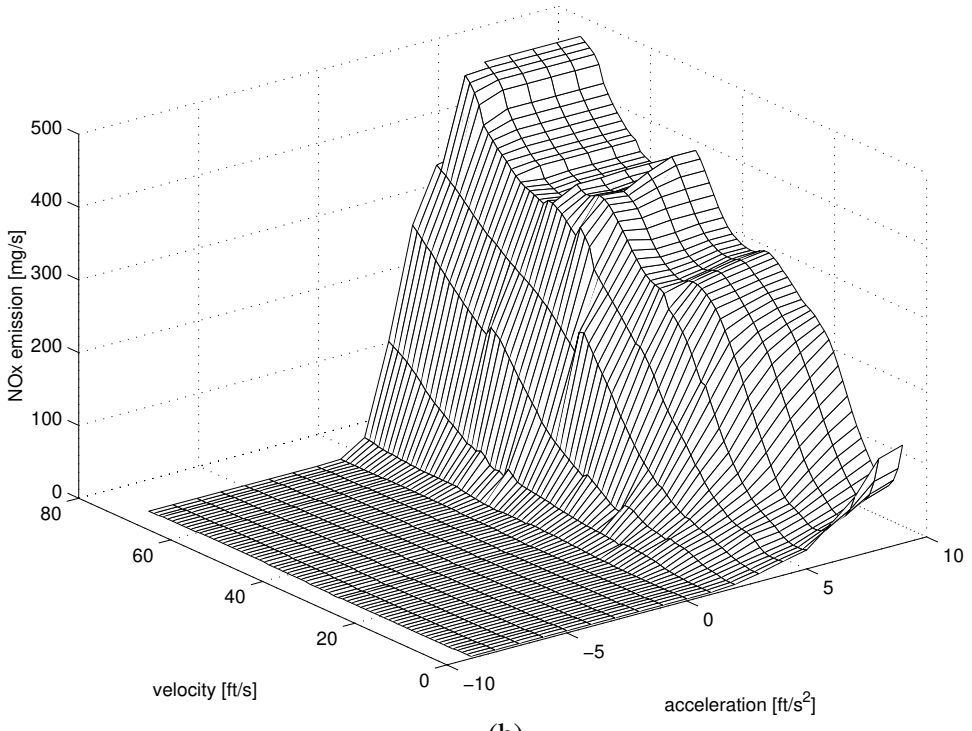

(b)

Figure 13: Maps for (a) CO emission and (b) NO_x emission indexed by velocity and acceleration.

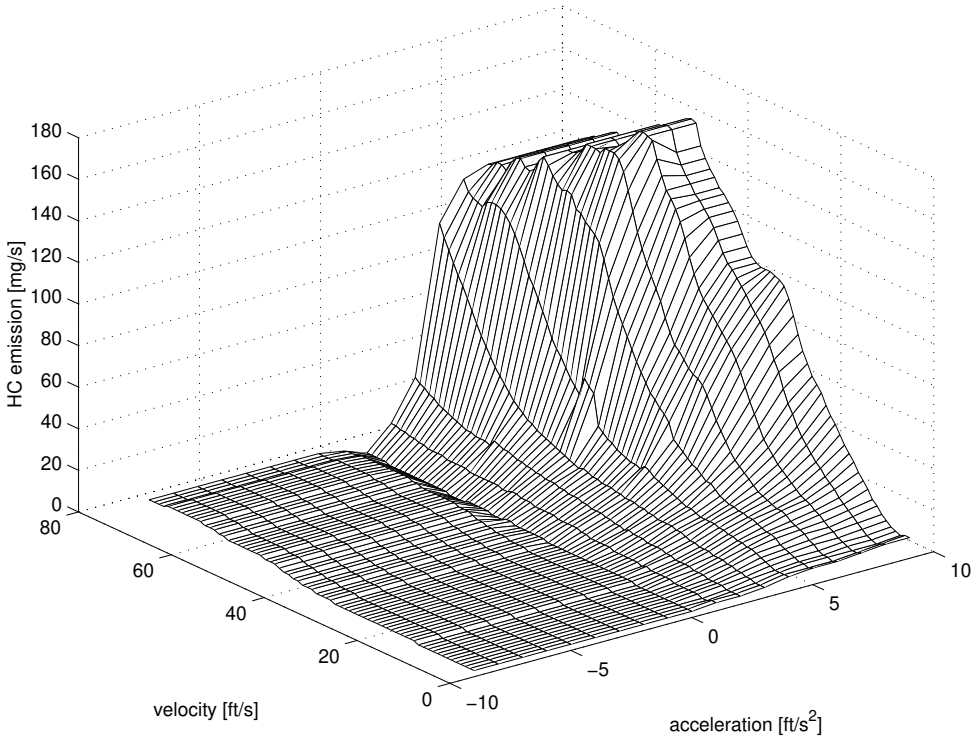

(c)

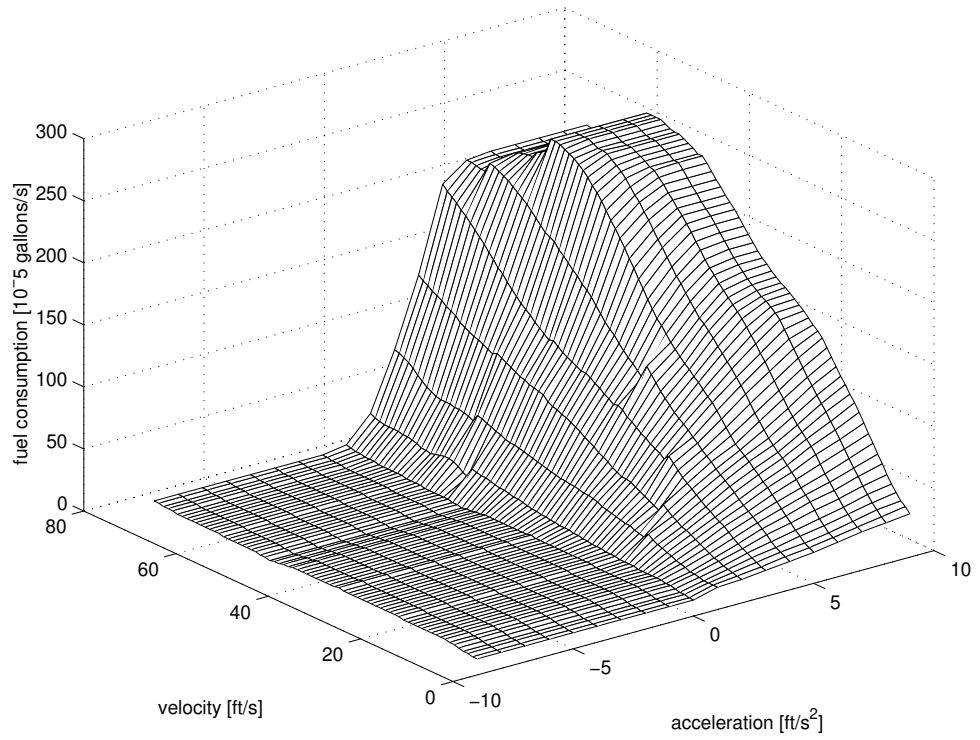

(d)

Figure 13: Maps for (c) HC emission and (d) fuel consumption indexed by velocity and acceleration.

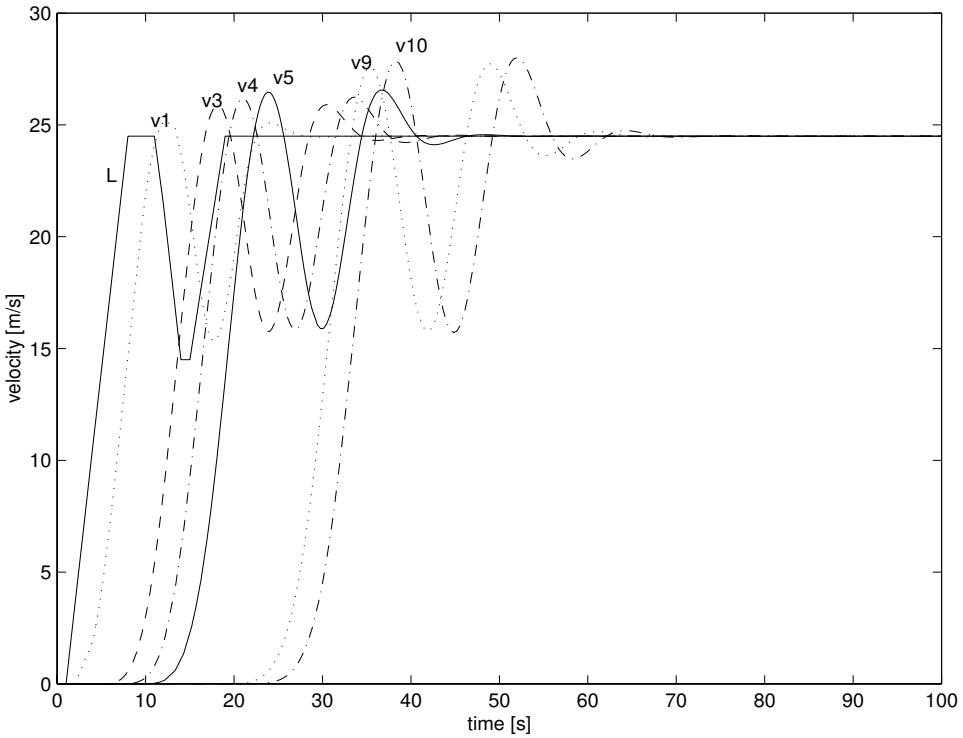

Figure 14: 10 manually driven vehicles follow a rapidly accelerating leader. Velocity response of leader (L), first vehicle (v1) and vehicles 3-5 (v3-v5) and 9,10 (v9, 10).

CO emission	24.6%
NO_x emission	47.3%
HC emission	3.8%
Fuel consumption	7.3%

Table 1: Percentage savings in pollution emission and fuel consumption for mixed traffic over manual traffic.

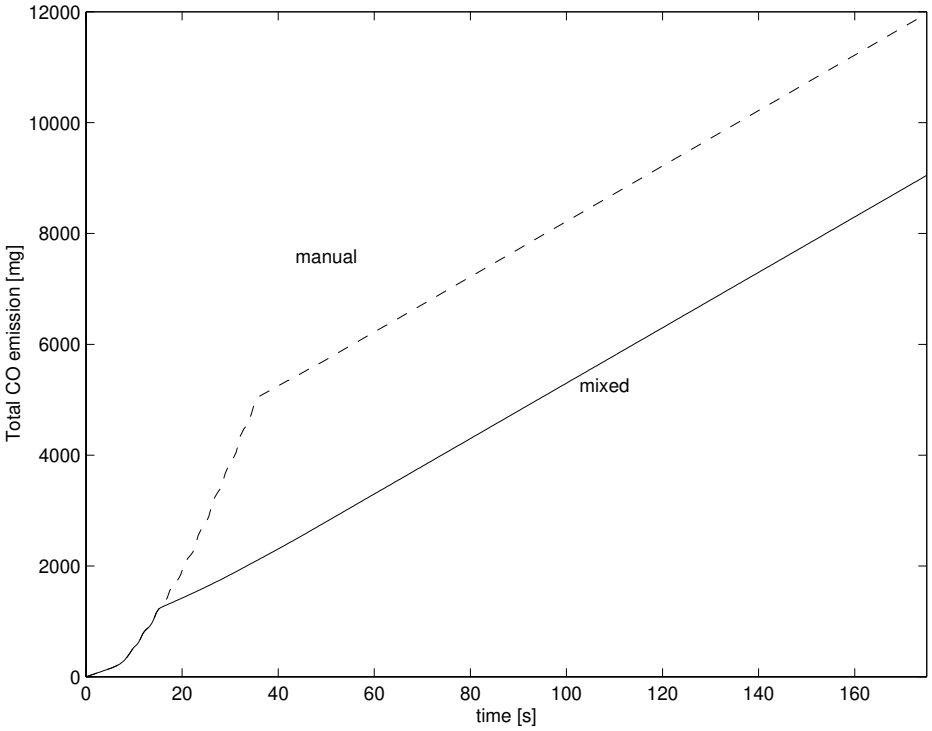

(a)

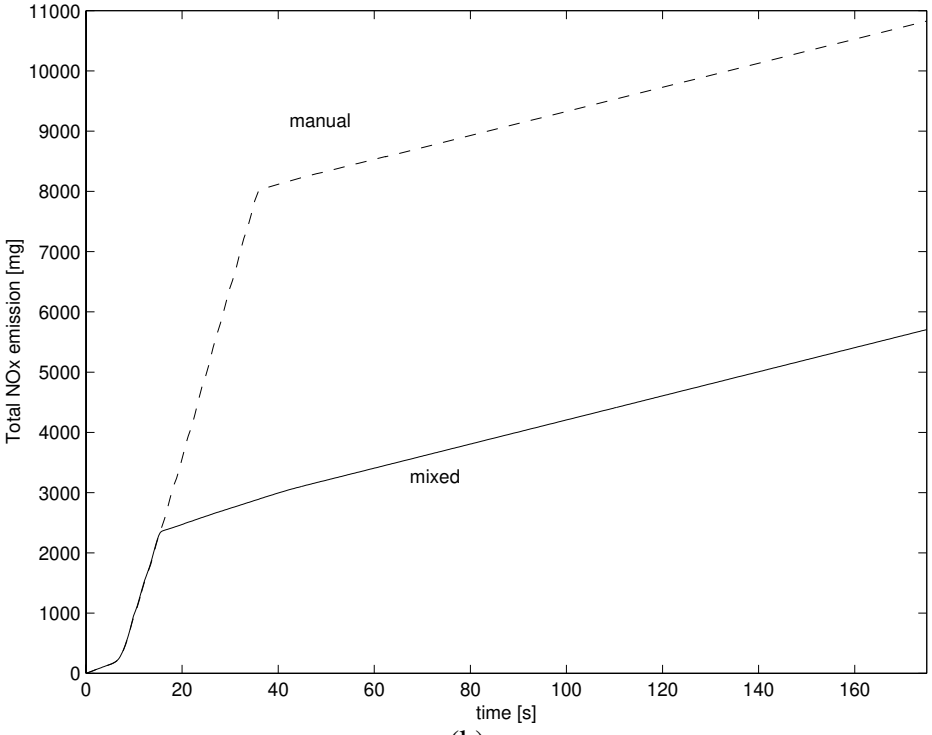

(b)

Figure 15: Total (a) CO emission and (b) NO_x emission from a string of 10 vehicles. Manual is when all vehicles are manually driven (Pipes model). Mixed is when the 4^{th} vehicle is semi-automated.

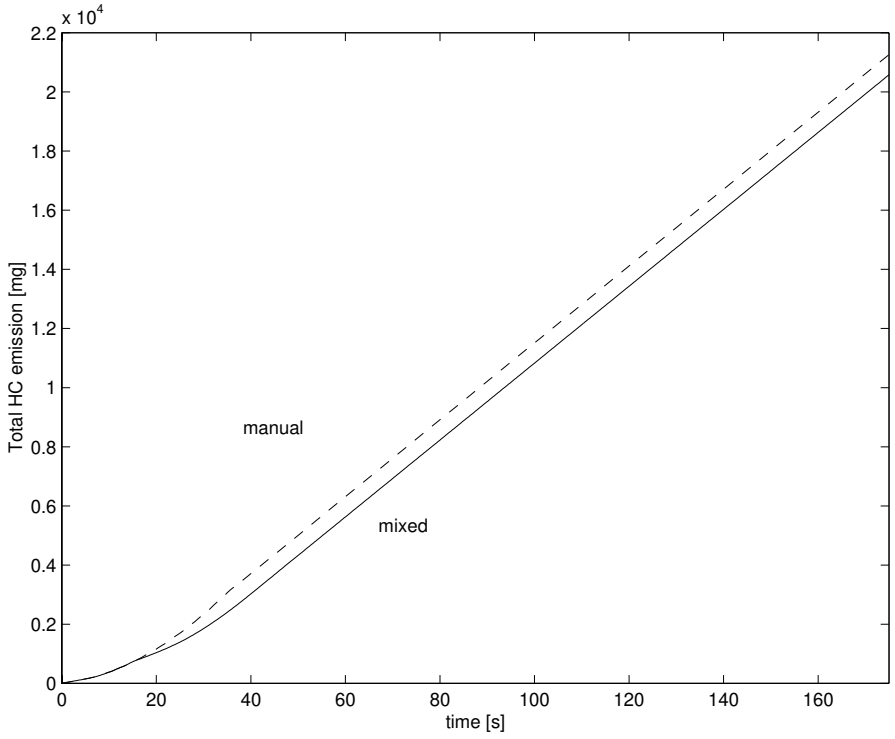

(c)

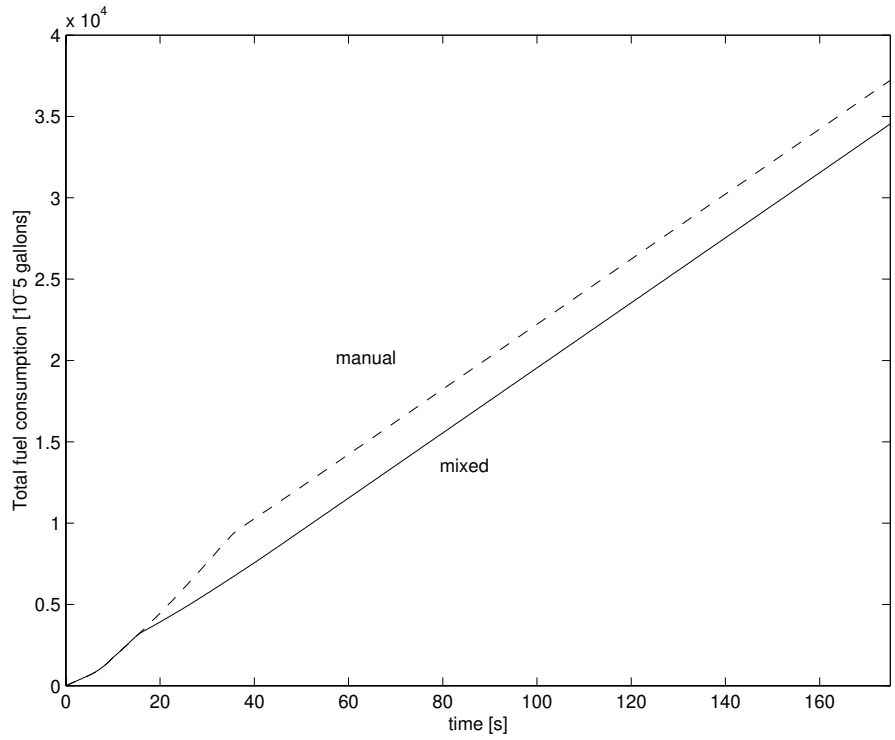

(d)

Figure 15: Total (c) HC emission and (d) fuel consumption from a string of 10 vehicles. Manual is when all vehicles are manually driven (Pipes model). Mixed is when the 4th vehicle is semi-automated.

4 Conclusions

In this paper we analyzed and simulated mixed manual/semi-automated traffic. Based on our findings, we can conclude the following:

- Semi-automated vehicles in mixed traffic do not contribute to the slinky effect phenomena during smooth transients.

- Semi-automated vehicles in mixed traffic smooth traffic flow by filtering the response of rapidly accelerating lead vehicles.

- The presence of semi-automated vehicles in mixed traffic improves air pollution levels and fuel savings during transients caused by rapid acceleration maneuvers.

References

[1] P. Ioannou and T. Xu, "Throttle and Brake Control", *IVHS Journal,* vol. 1(4), pp. 345-377, 1994

[2] P. Ioannou and A. Bose, "Evaluation of Mixed Automated/Manual Traffic", USC CATT Report No. 97-09-10, September 1997

[3] A. Bose and P. Ioannou, "Issues and Analysis of Mixed Semi-Automated/Manual Traffic", SAE Technical Paper Series No.981943, 1998

[4] Consumers Reports Online, September 1998

[5] M. J. Barth, "The Effect of AHS on the Environment", *Automated Highway Systems*, ed. P. Ioannou, Plenum Press, New York, 1997

[6] S. Sheikholeslam and C. A. Desoer, "Longitudinal Control of a Platoon of Vehicles with no Communication of Lead Vehicle Information", *Proceedings of the 1991 American Control Conference,* Boston, MA, pp. 3102-3106

[7] C. A. Desoer and M. Vidyasagar, *Feedback Systems: Input-Output Properties*, Academic Press Inc., New York, 1975

[8] L. A. Pipes, "An Operational Analysis of Traffic Dynamics", *J. of Applied Physics,* vol.24, pp. 271-281, 1953

[9] P. E. Chandler, R. Herman and E. W. Montroll, "Traffic Dynamics: Studies in Car Following", *Operations Research,* vol. 6, pp. 165-184, 1958

[10] J. S. Tyler, "The Characteristics of Model Following Systems as Synthesized by Optimal Control", *IEEE Transactions on Automatic Control,* vol. AC-9, pp. 485-498

[11] G.A. Bekey, G.O. Burnham and J. Seo, "Control Theoretic Models of Human Drivers in Car Following", *Human Factors,* vol. 19, pp. 399-413, 1977

[12] G.O. Burnham, J. Seo and G.A. Bekey, "Identification of Human Driver Models in Car Following", *IEEE Transactions on Automatic Control,* vol. 19, pp. 911-915, 1974

[13] FHWA's TRAF Simulation Models Emission Maps

[14] M. J. Barth, "Integrating a Modal Emissions Model into Various Transportation Modeling Frameworks", *ASCE Conference Proceedings*, 1997

[15] R. J. Walker and C. J. Harris, “A Multi-Sensor Fusion System for a Laboratory Based Autonomous Vehicle”, *Intelligent Autonomous Vehicles IFAC Workshop*, Southampton U.K., 1993, pp. 105-110
[16] *Special Report 209:* Highway Capacity Manual 1985, TRB, National Research Council, Washington D.C. 1985
[17] D. Swaroop and J.K. Hendrick, “String Stability of Interconnected Systems”, *IEEE Trans. on Automatic Control,* vol. 41, No. 3, pp. 349-357, 1996
[18] H. Raza and P. Ioannou, “Macroscopic Modeling of Automated Highway Systems" 36th IEEE Conference on Decision and Control, San Diego, California, Dec. 10-12, 1997, pp.4764-4770.